Carbon−Nitrogen Bond Cleavage in an $\eta^2(N,C)$-Pyridine Complex Induced by Intramolecular Metal-to-Ligand Alkyl Migration: Models for Hydrodenitrogenation Catalysis

Steven D. Gray, Keith J. Weller, Michael A. Bruck, Paula M. Briggs, and David E. Wigley*

Contribution from the Carl S. Marvel Laboratories of Chemistry, Department of Chemistry, University of Arizona, Tucson, Arizona 85721

Received April 19, 1995[⊗]

Abstract: The reaction of the $\eta^2(N,C)$-pyridine complex $[\eta^2(N,C)$-2,4,6-$NC_5{}^tBu_3H_2]Ta(OAr)_2Cl$ (**1**, Ar = 2,6-$C_6H_3{}^iPr_2$) with $LiBEt_3H$ affords the C−N bond scission product $Ta(=NC^tBu{=}CHC^tBu{=}CHCH^tBu)(OAr)_2$ (**2**). The reactions of $[\eta^2(N,C)$-2,4,6-$NC_5{}^tBu_3H_2]Ta(OAr)_2Cl$ (**1**) with carbon nucleophiles RLi or RMgX provide the alkyl derivatives $[\eta^2(N,C)$-2,4,6-$NC_5{}^tBu_3H_2]Ta(OAr)_2R$ [R = Me (**3**), Et (**4**), ^{n}Pr (**5**), ^{n}Bu (**6**), and CH_2SiMe_3 (**7**)]. Complexes **3**−**6** represent the kinetic products of the reaction since upon their thermolysis, alkyl migration from metal to ligand occurs and the C−N bond cleavage compounds $Ta(=NC^tBu{=}CHC^tBu{=}CHC^tBuR)(OAr)_2$ [R = Me (**8**), Et (**9**), ^{n}Pr (**10**), ^{n}Bu (**11**)] are formed. Kinetic and mechanistic studies of the **3** → **8** rearrangement reveal that methyl migration is strictly *intra*molecular. Further studies of $Ta(=NC^tBu{=}CHC^tBu{=}CHC^tBuMe)(OAr)_2$ (**8**) reveal that this complex subsequently rearranges to afford the eight-membered metallacycle $Ta(=NC^tBu{=}CHC^tBu{=}CHC^tBuHCH_2)(OAr)_2$ (**12**), which further decomposes to give the metallapyridine dimer $[Ta(\mu\text{-}NC^tBu{=}CHC^tBu{=}CH)(OAr)_2]_2$ (**13**) and ^{t}BuCH=CH_2. Synthetic and mechanistic studies on the **8** → **12** → **13** rearrangement reveal the source of the ^{t}BuCH=CH_2 through labeling experiments, allow the isolation of an adduct of **12**, *viz.* $Ta(=NC^tBu{=}CHC^tBu{=}CHC^tBu\text{-}HCH_2)(OAr)_2{\cdot}2NCMe$ (**12-NCMe**), and suggest a mechanistic scheme to account for these rearrangements. Complexes **2**, **4**, and **13** have been structurally characterized. $Ta(=NC^tBu{=}CHC^tBu{=}CHCH^tBu)(OAr)_2$ (**2**) crystallizes in the monoclinic space group $P2_1/n$ (No. 14) and displays a highly localized metallacyclic structure with an imido nitrogen linkage characterized by a Ta−N−C angle of 145.7(6)°. $[\eta^2(N,C)$-2,4,6-$NC_5{}^tBu_3H_2]Ta(OAr)_2Et$ (**4**) crystallizes in the monoclinic space group $P2_1/n$ (No. 14) and is characterized by an interruption of aromaticity to the heterocyclic ring through a 1,3-diene-like π electron localization. Metallapyridine $[Ta(\mu\text{-}NC^tBu{=}CHC^tBu{=}CH)(OAr)_2]_2$ (**13**) crystallizes in the triclinic space group $P\bar{1}$ (No. 2) and reveals an extremely crowded structure with a π localized, formal $[\mu\text{-}NC^tBu{=}CHC^tBu{=}CH]^{3-}$ μ-imido ligand. The reactions of this model system delineate one process by which heterocyclic C−N bonds are cleaved and offer new insight as to how nitrogen heterocycles may be further degraded *after* C−N bond cleavage in hydrodenitrogenation catalysis.

Introduction

Performing catalytic hydrodenitrogenation (HDN) on petroleum and coal-derived liquids is essential to reduce the emissions of NO_x upon burning these fuels and since nitrogen-containing compounds seriously reduce the activity of hydrocracking and reforming catalysts.[1−5] Of all the nitrogen compounds subject to HDN catalysis, the *basic heterocyclic* compounds, e.g. pyridines and quinolines, are among the most difficult to process.[6−9] While the *hydrogenation* of pyridine rings is comparatively facile under standard HDN conditions (300−450 °C, ≥2000 psi H_2), the subsequent C−N bond *hydrogenolysis* reactions are considerably more difficult.[8−13] In addition, the greater C−N bond energies as compared to C−S bonds (by 3−9 kcal mol^{-1})[6] usually make HDN less efficient than hydrodesulfurization (HDS) catalysis under most conditions.[1,2]

The mechanistic details surrounding metal-mediated C−N bond cleavage[14−22] are particularly important to understanding HDN since the metal's role in promoting this reaction remains

[⊗] Abstract published in *Advance ACS Abstracts*, October 1, 1995.

(1) Gary, J. H.; Handwerk, G. E. *Petroleum Refining: Technology and Economics*, 3rd ed.; Marcel Dekker, Inc.: New York, 1993.
(2) Satterfield, C. N. *Heterogeneous Catalysis in Industrial Practice*, 2nd ed.; McGraw-Hill, Inc.: New York, 1991.
(3) Angelici, R. J. In *Encyclopedia of Inorganic Chemistry*; King, R. B., Ed.; John Wiley and Sons: New York, 1994; Vol. 3, pp 1433−1443.
(4) Ho, T. C. *Catal. Rev.-Sci. Eng.* **1988**, *30*, 117.
(5) Ledoux, M. J. In *Catalysis*; The Chemical Society: London, 1988; Vol. 7, pp 125−148.
(6) Katzer, J. R.; Sivasubramanian, R. *Catal. Rev.-Sci. Eng.* **1979**, *20*, 155.
(7) Laine, R. M. *Catal. Rev.-Sci. Eng.* **1983**, *25*, 459.
(8) Laine, R. M. *Ann. N.Y. Acad. Sci.* **1983**, *415*, 271.
(9) Fish, R. H. *Ann. N.Y. Acad. Sci.* **1983**, *415*, 292.
(10) Fish, R. H.; Michaels, J. N.; Moore, R. S.; Heinemann, H. *J. Catal.* **1990**, *123*, 74.
(11) Fish, R. H.; Thormodsen, A. D.; Moore, A. D.; Perry, D. L.; Heinemann, H. *J. Catal.* **1986**, *102*, 270.
(12) Satterfield, C. N.; Modell, M.; Wilkers, J. A. *Ind. Eng. Chem. Process Des. Dev.* **1980**, *19*, 154.
(13) Satterfield, C. N.; Yang, S. H. *Ind. Eng. Chem. Process Des. Dev.* **1984**, *23*, 11.
(14) Laine, R. M. *New J. Chem.* **1987**, *11*, 543.
(15) Satterfield, C. N.; Cocchetto, J. F. *Ind. Eng. Chem. Process Des. Dev.* **1981**, *20*, 53.
(16) Olalde, A.; Perot, G. *Appl. Catal.* **1985**, *13*, 373.

0002-7863/95/1517-10678$09.00/0

unresolved.[4,23] Several well-characterized C−S bond scission reactions in thiophene have been reported in HDS model studies,[24−31] however metal-mediated C−N bond scissions have been limited to aliphatic amine substrates in systems not easily amenable to study.[32−36] Recently, we reported the reaction of hydride (from $LiBEt_3H$) with the $\eta^2(N,C)$-pyridine complex $[\eta^2(N,C)$-2,4,6-$NC_5{}^tBu_3H_2]Ta(OAr)_2Cl$ (Ar = 2,6-$C_6H_3{}^iPr_2$) that resulted in C−N bond scission and formation of the ring-opened, metallacyclic complex $Ta(=NC^tBu=CHC^tBu=CHCH^tBu)(OAr)_2$.[37,38] This reaction affords a unique opportunity to examine mechanistic aspects of an elusive C−N bond cleavage and perhaps elucidate the role of the metal atom in the reaction.

In this paper, we report details of the reactions of the $\eta^2(N,C)$-pyridine complex $[\eta^2(N,C)$-2,4,6-$NC_5{}^tBu_3H_2]Ta(OAr)_2Cl$ with hydride and carbon nucleophiles, define one mechanism of C−N bond cleavage, and uncover a subsequent rearrangement of the resulting metallacyclic complex. These reactions offer new insight in HDN-related processes, including the manner by which nitrogen heterocycles may further degrade *after* C−N *bond scission*.[39] A portion of these results have been communicated.[37]

Results

Reaction of an $\eta^2(N,C)$-Pyridine Complex with Hydride: Regioselective Carbon−Nitrogen Bond Cleavage. Upon reacting $[\eta^2(N,C)$-2,4,6-$NC_5{}^tBu_3H_2]Ta(OAr)_2Cl$ (**1**)[40] with 1 equiv of $LiBEt_3H$ (THF, 20 h, room temperature), red crystalline **2** can be isolated in low yield after appropriate workup (Scheme 1). Examining the entire reaction mixture by ^1H NMR reveals that the conversion of **1** to **2** proceeds in approximately 50% yield under these conditions with several, unidentifiable species and a small amount of unreacted **1** also present. The NMR spectra of **2** are consistent with hydride addition occurring at the metal-bound carbon of the $\eta^2(N,C)$-pyridine ligand. In particular, the δ 5.93 and 5.55 singlets assigned as the pyridine ring protons in the ^1H NMR spectrum of **1** are replaced by a δ 5.91 singlet [H(4)] and a δ 5.84 doublet [H(2), $^3J_{HH}$ = 10.5 Hz] which is coupled to a new δ 4.51 signal [H(1)] in the spectrum of **2** (C_6D_6). The notion that hydride addition has occurred at the metal-bound carbon is supported by the ^1H NMR data of the labeled complex, **2-*d*$_1$** (prepared using $LiBEt_3D$), in which the δ 4.51 resonance is absent and the H(2) signal collapses to a broad singlet. Accordingly, the resonance for C(1) in the gated $^{13}C\{^1H\}$ NMR spectrum of **2** appears as a δ 103.4 doublet with a C−H coupling constant ($^1J_{CH}$ = 135.0 Hz), suggesting sp^3 hybridization of this carbon. While these NMR data and the elemental analysis of **2** support its formulation as $(NC_5{}^tBu_3H_3)Ta(OAr)_2$, the bonding mode of the nitrogen ligand could not be established unambiguously from its spectroscopic properties.

Scheme 1

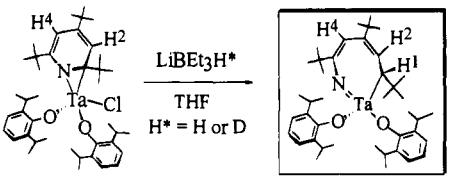

1 **2**

Structural Study of $Ta(=NC^tBu=CHC^tBu=CHCH^tBu)(OAr)_2$ (2). Red, single crystals of **2** suitable for an X-ray structural determination were grown from concentrated pentane solutions at −35 °C. Tables 1 and 2 present details of the structural study and selected structural data, respectively. Figure 1 presents the molecular structure of **2** and provides the dramatic evidence that the carbon−nitrogen bond of the $\eta^2(N,C)$-pyridine ligand in **1** has been cleaved upon hydride addition. The disconnection between the N and C(1) of the former pyridine ligand and the resulting seven-membered metallacyclic structure of $Ta(=NC^tBu=CHC^tBu=CHCH^tBu)(OAr)_2$ (**2**) are unambiguous, confirming that net hydride addition has occurred to the pyridine C(1). (The hydrogen attached to C(1) has been located in the difference map.) In the metallaaziridine description[41−44] of $[\eta^2(N,C)$-2,4,6-$NC_5{}^tBu_3H_2]Ta(OAr)_2Cl$ (**1**), the former *amido* nitrogen[45,46] has been transformed into a formal *imido* linkage upon hydride attack as depicted in Scheme 1. The formation of the strong metal-ligand multiple bond in **2** no doubt represents a major driving force for this reaction, since a strong C−N bond is cleaved in this process.

The local coordination about tantalum is a distorted tetrahedron with L−Ta−L angles ranging from 87.6(3)° for C(1)−Ta−N to 118.1(3)° for N−Ta−O(20), Table 2. Thus, the constraints of the metallacycle allow all other L−Ta−L angles in the molecule to increase above the 109° expected for a tetrahedron. The Ta−N−C(5) bond angle of 145.7(6)° renders

(17) Satterfield, C. N.; Modell, M.; Hites, R. A.; Declerck, C. J. *Ind. Eng. Chem. Process Des. Dev.* **1978**, *17*, 141.
(18) Yang, S. H.; Satterfield, C. N. *J. Catal.* **1983**, *81*, 168.
(19) Yang, S. H.; Satterfield, C. N. *Ind. Eng. Chem. Process Des. Dev.* **1984**, *23*, 20.
(20) Satterfield, C. N.; Smith, C. M.; Ingalls, M. *Ind. Eng. Chem. Process Des. Dev.* **1985**, *24*, 1000.
(21) Satterfield, C. N.; Gültekin, S. *Ind. Eng. Chem. Process Des. Dev.* **1981**, *20*, 62.
(22) Vivier, L.; Dominguez, V.; Perot, G.; Kasztelan, S. *J. Mol. Catal.* **1991**, *67*, 267.
(23) Prins, R.; de Beer, V. H. J.; Somorjai, G. A. *Catal. Rev.-Sci. Eng.* **1989**, *31*, 1.
(24) Ogilvy, A. E.; Skaugset, A. E.; Rauchfuss, T. B. *Organometallics* **1988**, *7*, 1171.
(25) Chen, J.; Daniels, L. M.; Angelici, R. J. *J. Am. Chem. Soc.* **1990**, *112*, 199.
(26) Chen, J.; Daniels, L. M.; Angelici, R. J. *J. Am. Chem. Soc.* **1991**, *113*, 2544.
(27) Chen, J.; Daniels, L. M.; Angelici, R. J. *Polyhedron* **1990**, *9*, 1883.
(28) Jones, W. D.; Dong, L. *J. Am. Chem. Soc.* **1991**, *113*, 559.
(29) Dong, L.; Duckett, S. B.; Ohman, K. F.; Jones, W. D. *J. Am. Chem. Soc.* **1992**, *114*, 151.
(30) Jones, W. D.; Chin, R. M. *Organometallics* **1992**, *11*, 2698.
(31) Spies, G. H.; Angelici, R. J. *Organometallics* **1987**, *6*, 1897.
(32) Adams, R. D.; Chen, G. *Organometallics* **1993**, *12*, 2070.
(33) Adams, R. D.; Tanner, J. T. *Appl. Organomet. Chem.* **1992**, *6*, 449.
(34) Kabir, S. E.; Day, M.; Irving, M.; McPhillips, T.; Minassian, H.; Rosenberg, E.; Hardcastle, K. I. *Organometallics* **1991**, *10*, 3997.
(35) Laine, R. M.; Thomas, D. W.; Cary, L. W.; Buttrill, S. E. *J. Am. Chem. Soc.* **1978**, *100*, 6527.
(36) Laine, R. M.; Thomas, D. W.; Cary, L. W. *J. Am. Chem. Soc.* **1982**, *104*, 1763.
(37) Gray, S. D.; Smith, D. P.; Bruck, M. A.; Wigley, D. E. *J. Am. Chem. Soc.* **1992**, *114*, 5462.
(38) Gray, S. D.; Fox, P. A.; Kingsborough, R. P.; Bruck, M. A.; Wigley, D. E. *ACS Prepr. Div. Petrol. Chem.* **1993**, *39*, 706.
(39) Choi, J.-G.; Brenner, J. R.; Colling, C. W.; Demczyk, B. G.; Dunning, J. L.; Thompson, L. T. *Catal. Today* **1992**, *15*, 201.
(40) Smith, D. P.; Strickler, J. R.; Gray, S. D.; Bruck, M. A.; Holmes, R. S.; Wigley, D. E. *Organometallics* **1992**, *11*, 1275.
(41) Durfee, L. D.; Fanwick, P. E.; Rothwell, I. P.; Folting, K.; Huffman, J. C. *J. Am. Chem. Soc.* **1987**, *109*, 4720.
(42) Mayer, J. M.; Curtis, C. J.; Bercaw, J. E. *J. Am. Chem. Soc.* **1983**, *105*, 2651.
(43) Durfee, L. D.; Hill, J. E.; Kerschner, J. L.; Fanwick, P. E.; Rothwell, I. P. *Inorg. Chem.* **1989**, *28*, 3095.
(44) Chiu, K. W.; Jones, R. A.; Wilkinson, G.; Galas, A. M. R.; Hursthouse, M. B. *J. Chem. Soc., Dalton Trans.* **1981**, 2088.
(45) Covert, K. J.; Neithamer, D. R.; Zonnevylle, M. C.; LaPointe, R. E.; Schaller, C. P.; Wolczanski, P. T. *Inorg. Chem.* **1991**, *30*, 2494.
(46) Neithamer, D. R.; Párkányi, L.; Mitchell, J. F.; Wolczanski, P. T. *J. Am. Chem. Soc.* **1988**, *110*, 4421.

Table 1. Details of the X-ray Diffraction Studies for Ta(=NC^{t}Bu=CHC^{t}Bu=CHCH^{t}Bu)(OAr)$_2$ (**2**), [η^2(*N,C*)-2,4,6-NC$_5$^{t}Bu$_3$H$_2$]Ta(OAr)$_2$Et (**4**), and [Ta(μ-NC^{t}Bu=CHC^{t}Bu=CH)(OAr)$_2$]$_2$ (**13**)

parameter	Ta(=NC^{t}Bu=CHC^{t}Bu=CHCH^{t}Bu)-(OAr)$_2$ (**2**)	[η^2(*N,C*)-2,4,6-NC$_5$^{t}Bu$_3$H$_2$]-Ta(OAr)$_2$Et (**4**)	[Ta(μ-NC^{t}Bu=CHC^{t}Bu=CH)-(OAr)$_2$]$_2$ (**13**)
		Crystal Parameters	
molecular formula	$C_{41}H_{64}NO_2Ta$	$C_{43}H_{68}O_2NTa$	$C_{36}H_{54}O_2NTa$
formula weight	783.92	811.97	713.79
F(000)	1624	1688	732
crystal color	red	orange	red
space group	monoclinic $P2_1/n$ (No. 14)	monoclinic $P2_1/n$ (No. 14)	$P\bar{1}$ (No. 2)
unit cell volume, Å^3	4150.5	4351(9)	1730.9(3)
a, Å	21.150(2)	12.009(9)	13.2564(9)
b, Å	9.623(1)	19.690(14)	13.4315(9)
c, Å	21.519(2)	18.402(14)	11.9736(9)
α, deg	(90)	(90)	113.560(6)
β, deg	108.63(18)	90.78(2)	109.350(6)
γ, deg	(90)	(90)	99.526(6)
Z	4	4	2
D(calc), g cm^{-3}	1.25	1.24	1.37
crystal dimensions, mm	0.07 × 0.22 × 0.50	0.51 × 0.50 × 0.10	0.17 × 0.28 × 0.37
ω width, deg	0.30	0.30	0.16
abs coeff, cm^{-1}	26.5	25.3	31.7
data collection temp, °C	20 ± 1	23 ± 1	20 ± 1
		Data Collection	
diffractometer	Syntex P2$_1$, Crystal Logics	Syntex P2$_1$, Crystal Logics	Enraf-Nonius CAD4
monochromator	graphite crystal, incident beam	graphite crystal, incident beam	graphite crystal, incident beam
attenuator	none	none	Zr foil, factor 13.6
Mo Kα radiation, λ, Å	0.71073	0.71073	0.71073
2θ range, deg	0−50	0−50	0−50
octants collected	$+h,+k,\pm l$	$+h,+k,\pm l$	$+h,\pm k,\pm l$
scan type	ω−2θ	ω−2θ	ω−2θ
scan speed, deg min^{-1}	3	3	2−7
scan width, deg	2θKα_1 − 1.3° to 2θKα_2 + 1.6°	2θKα_1 − 1.3° to 2θKα_2 + 1.6°	0.8 + 0.34 tanθ
total no. of reflns measd	8037 (7324 unique)	8220 (7566 unique)	6403 (6085 unique)
corrections	Lorentz−polarization reflection averaging (agreement on I = 2.1%) Ψ-scan absorption	Lorentz−polarization reflection averaging (agreement on I = 5.2%) Ψ-scan absorption	Lorentz−polarization reflection averaging (agreement on I = 1.6%) Ψ-scan absorption
		Solution and Refinement	
solution	Patterson method	Patterson method	Patterson method
refinement	full-matrix least-squares	full-matrix least-squares	full-matrix least-squares
no. of reflns used in refinement; $I > 3\sigma(I)$	4091	4784	5542
no. of parameters refined	415	426	361
R	0.040	0.040	0.027
R_w	0.049	0.050	0.036
esd of obs of unit wt	1.23	1.40	1.34
convergence, largest shift	0.29σ	0.23σ	0.32σ
Δ/σ(max), e^{-1}/Å^3	0.70(11)	1.03(11)	2.21(9)
Δ/σ(min), e^{-1}/Å^3	−0.21(11)	−0.16(11)	−0.11(9)
computer hardware	VAX	VAX	VAX
computer software	MolEN	MolEN	MolEN

2 one of the most strongly bent terminal imido complexes ever structurally characterized,[47] though this angle is not highly unusual for chelating imido ligands.[48,49] In the case of Ta(=NC^{t}Bu=CHC^{t}Bu=CHCH^{t}Bu)(OAr)$_2$ (**2**), it seems reasonable to propose the Ta−N−C bend arises from the metallacyclic structure, yet despite this distortion the Ta-N bond length of 1.770(8) Å in **2** compares well with other d^0 Ta=NR functional groups.[47] The metallacycle is clearly π-localized as represented in Scheme 1.

Mechanistic Considerations of Carbon−Nitrogen Bond Cleavage with Hydride Nucleophiles. Of the possible scenarios that could account for the conversion of the η^2(*N,C*)-pyridine complex **1** to the C−N bond cleavage product **2**, perhaps the most significant question to address is the extent to which the metal center mediates the reaction. The most simple mechanism involves a direct, *exo* hydride attack on the bound carbon of the pyridine complex (Scheme 2). Nucleophilic attack of the hydride at the metal to form an unstable hydride complex, followed by an *endo* hydride transfer from the metal to the pyridine ligand also represents a viable pathway for C−N bond scission (Scheme 2). An examination of the molecular structure of **2** reveals that the hydride has apparently added to the face of the pyridine ligand directed away from the metal center (Figure 2). Thus it *appears* that an *exo* mechanism for hydride transfer to the pyridine ligand has occurred. However, we note that *endo* attack cannot be ruled out from the molecular structure of **2** alone, as simple rotation about the Ta−C(1) bond and the Ta−N−C(5) linkage of the metallacycle of an *endo*-

(47) Wigley, D. E. *Prog. Inorg. Chem.* **1994**, *42*, 239.
(48) Minelli, M.; Kuhlman, R. L.; Shaffer, S. J.; Chiang, M. Y. *Inorg. Chem.* **1992**, *31*, 3891.
(49) Minelli, M.; Carson, M. R.; Whisenhunt, D. W., Jr.; Imhof, W.; Huttner, G. *Inorg. Chem.* **1990**, *29*, 4801.

Table 2. Selected Bond Distances (Å) and Bond Angles (deg) in Ta(=NC^{t}Bu=CHC^{t}Bu=CHCH^{t}Bu)(OAr)$_2$ (**2**)[a]

Bond Distances			
Ta−N	1.779(8)	C(3)−C(4)	1.49(1)
Ta−C(1)	2.16(1)	C(4)−C(5)	1.34(1)
Ta−O(10)	1.877(6)	C(5)−N	1.40(1)
Ta−O(20)	1.909(6)	O(20)−C(21)	1.39(1)
C(1)−C(2)	1.51(1)	O(10)−C(11)	1.38(1)
C(2)−C(3)	1.35(1)		
Bond Angles			
Ta−N−C(5)	145.7(6)	C(1)−Ta−O(10)	110.5(3)
Ta−C(1)−C(2)	89.2(6)	C(1)−Ta−O(20)	115.1(3)
Ta−O(10)−C(11)	160.4(6)	O(10)−Ta−O(20)	112.8(3)
Ta−O(20)−C(21)	154.5(6)	C(1)−C(2)−C(3)	129.7(9)
N−Ta−C(1)	87.6(3)	C(2)−C(3)−C(4)	122.1(9)
N−Ta−O(10)	110.3(3)	C(3)−C(4)−C(5)	125.2(9)
N−Ta−O(20)	118.1(3)	N−C(5)−C(4)	118.5(9)

[a] Numbers in parentheses are estimated standard deviations in the least significant digits.

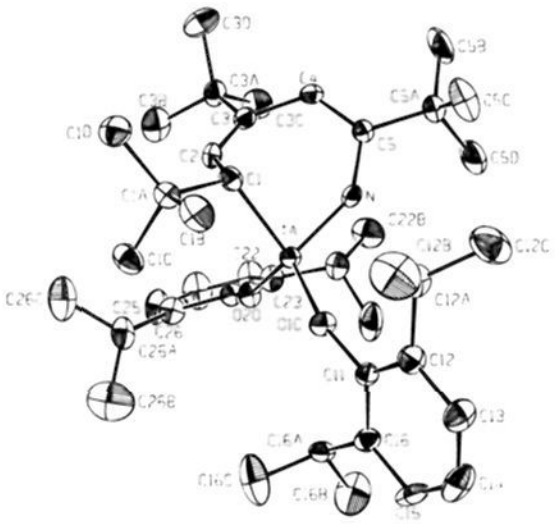

Figure 1. Molecular structure of Ta(=NC^{t}Bu=CHC^{t}Bu=CHCH^{t}Bu)-(OAr)$_2$ (**2**) with atoms represented as 20% ellipsoids.

Scheme 2

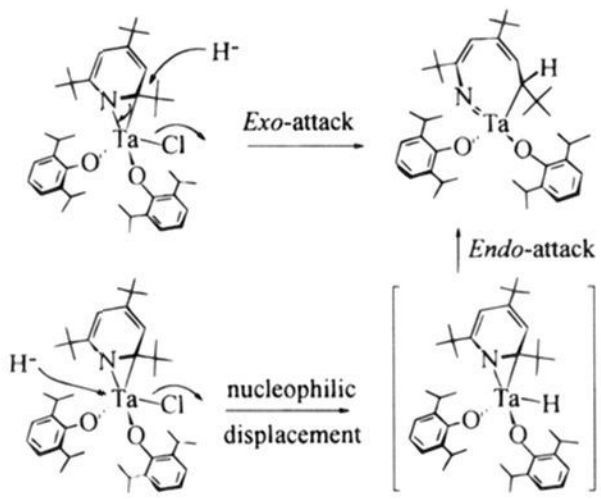

addition product, brought about by an "envelope ring flip", would result in an apparent *endo*-addition structure. This process is represented for both enantiomers of **2** in Scheme 3.

No identifiable intermediates could be detected spectroscopically in the complex reaction of **1** with LiBEt$_3$H, therefore attempts were made to prepare the purported $\eta^2(N,C)$-pyridine−hydride complex, $[\eta^2(N,C)$-2,4,6-NC$_5$^{t}Bu$_3$H$_2$]Ta(OAr)$_2$H, by other routes. If this species could be isolated and converted to the ring-opened complex **2** (under similar conditions as **1** is converted to **2**) or if **2** can be isolated from a reaction which unambiguously produced $[\eta^2(N,C)$-2,4,6-NC$_5$^{t}Bu$_3$H$_2$]Ta(OAr)$_2$H, then its intermediacy in the C−N bond cleavage reaction might be established. Numerous efforts to metathesize the chloride ion of $[\eta^2(N,C)$-2,4,6-NC$_5$^{t}Bu$_3$H$_2$]Ta(OAr)$_2$Cl (**1**) with more mild hydride sources such as Et$_3$SiH and ^{n}Bu$_3$SnH failed to produce any isolable tantalum hydride complex or **2** and instead led to either uncharacterizable products or no reaction. Further attempts to introduce a hydride ligand earlier in the cycloaddition synthesis of $[\eta^2(N,C)$-2,4,6-NC$_5$^{t}Bu$_3$H$_2$]Ta(OAr)$_2$Cl (**1**) also provided only starting material or uncharacterizable mixtures of products (see Experimental Section).

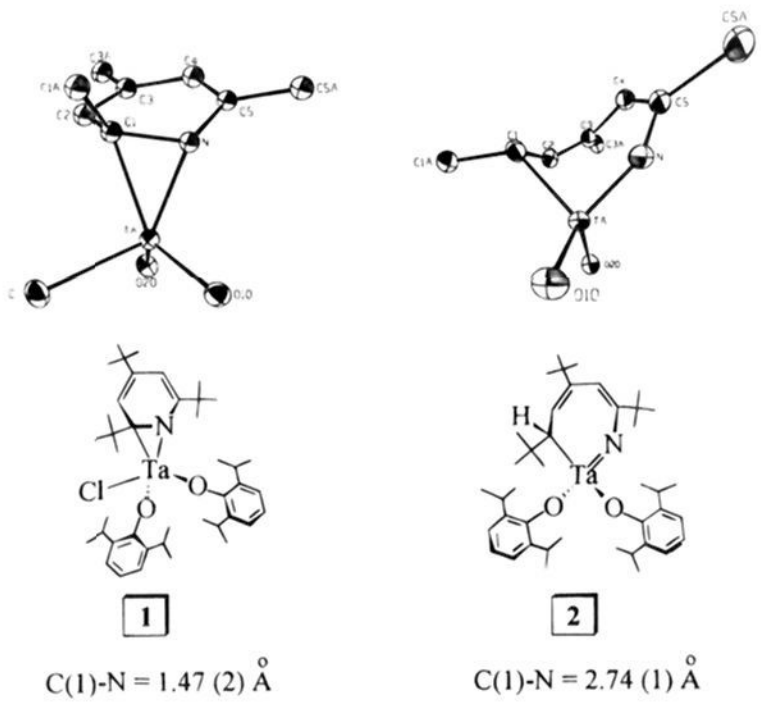

Figure 2. Structural comparisons of the local coordination in an $\eta^2(N,C)$-pyridine complex before $\{[\eta^2(N,C)$-2,4,6-NC$_5$^{t}Bu$_3$H$_2$]Ta(OAr)$_2$-Cl (**1**)$\}$ and after [Ta(=NC^{t}Bu=CHC^{t}Bu=CHCH^{t}Bu)(OAr)$_2$ (**2**)] hydride attack. The *exo* hydrogen bonded to C(1) in the structure of **2** was located in the difference map in the X-ray structure determination.

Scheme 3

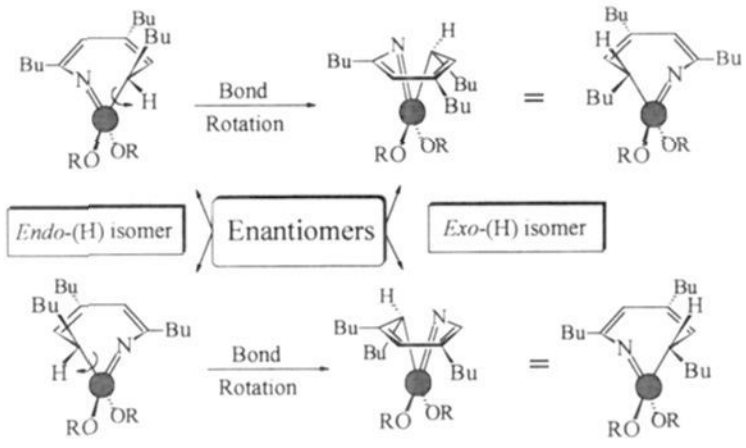

Finally, our attempts to address this question of *endo*- vs *exo*-hydride attack in Scheme 2 led us to examine the reactions of $[\eta^2(N,C)$-2,4,6-NC$_5$^{t}Bu$_3$H$_2$]Ta(OAr)$_2$Cl (**1**) with carbon nucleophiles. These reactions were deemed relevant for two reasons. First, given the inability to isolate or observe any tantalum hydride species in the C−N cleavage reaction of Scheme 1, the reactivity of **1** with other nucleophiles was an attractive prospect to establish the regioselectivity of attack. Second, attempts to generate a tantalum hydride species via β-H elimination in alkyl derivatives of the type $[\eta^2(N,C)$-2,4,6-NC$_5$^{t}Bu$_3$H$_2$]Ta(OAr)$_2$(CH$_2$CH$_2$R) were also an appealing possibility.

Reactions of an $\eta^2(N,C)$-Pyridine Complex with Carbon Nucleophiles: Isolation of the Alkyl Derivatives $[\eta^2(N,C)$-2,4,6-NC$_5$^{t}Bu$_3$H$_2$]Ta(OAr)$_2$R and Evidence for the Formation of an Intermediate Hydride Complex. Upon reacting $[\eta^2(N,C)$-2,4,6-NC$_5$^{t}Bu$_3$H$_2$]Ta(OAr)$_2$Cl (**1**) with 1 equiv of MeMgCl in benzene/THF, quantitative formation of the orange complex **3** is effected, although pure **3** is isolated only in moderate yields (ca. 70%) due to its extreme solubility (Scheme 4). The salient feature in the room temperature ^{1}H NMR spectrum of **3** is the broad singlet at δ 5.63 (C$_6$D$_6$) indicating

Scheme 4

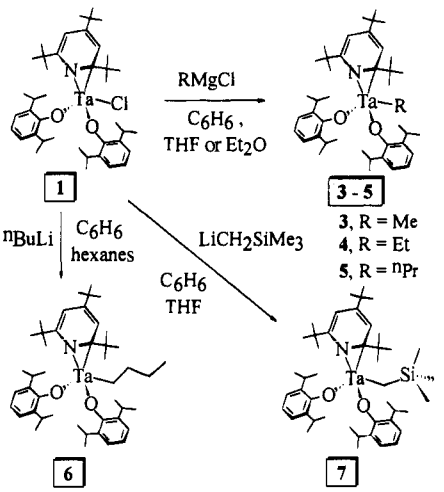

the *equivalence* of H(2) and H(4) of the $NC_5{}^tBu_3H_2$ ligand by some rearrangement process. The fact that the pyridine ring protons equilibrate clearly demonstrates that nucleophilic attack has occurred *at the metal center* and not the pyridine ligand; accordingly, **3** is formulated as the methyl complex $[\eta^2(N,C)$-2,4,6-$NC_5{}^tBu_3H_2]Ta(OAr)_2Me$.

Upon cooling toluene-d_8 solutions of **3** to −90 °C, the resonances for H(2) and H(4) decoalesce and the static $\eta^2(N,C)$-pyridine structure can be frozen out with resonances at δ 5.73 and 5.50. This observation leads to the approximate energy for the exchange process of 14.4 ± 0.2 kcal mol^{-1} at 25 °C. Additionally, the fact that the $NC_5{}^tBu_3H_2$ ligand in **3** does not exchange with pyridine and free 1,3,5-$NC_5{}^tBu_3H_2$ is not incorporated into $[\eta^2(N,C)$-2,4,6-$NC_5{}^tBu_3D_2]Ta(OAr)_2Me$ (**3-d_2**, *vide infra*) at probe temperature indicates that a dissociative pathway by which H(2) and H(4) equilibrate is *not* operative. We propose that a simple "ring-rocking" process is occurring in **3** by which pyridine *ortho* carbons alternately coordinate and then dissociate from the metal, as suggested in Figure 3, and that ring rocking proceeds via an intermediate possessing a molecular plane of symmetry. While the $\eta^1(N)$-pyridine intermediate suggested in Scheme 5 *could* account for the fluxional behavior of **3**, it is much more likely that a π complex $[\eta^{n>2}(N,C_{n-1})$-2,4,6-$NC_5{}^tBu_3H_2]Ta(OAr)_2Cl$ constitutes a lower energy intermediate. This suggestion is consistent with Wolczanski's EHMO calculations on hypothetical $(NC_5H_5)Ta(OH)_3$ that predict an energy ordering of $\eta^2(N,C) < \eta^6(\pi) < \eta^1(N)$ as indicated in Scheme 5.[45] Therefore the high-energy, "filled−filled" interaction between the pyridine lone pair and the d_{z^2} HOMO of the $Ta(OH)_3$ fragment in an $\eta^1(N)$ structure suggests π intermediates such as η^4 or η^6 are more reasonable. We note that steric effects do not preclude the η^6 intermediate indicated in Scheme 5, since the η^6-$C_6{}^tBu_3H_3$ arene congener of **3**, $(\eta^6$-$C_6{}^tBu_3H_3)Ta(OAr)_2Me$, has been fully characterized.[40]

The alkyl complexes $[\eta^2(N,C)$-2,4,6-$NC_5{}^tBu_3H_2]Ta(OAr)_2R$ [for R = Et (**4**), ^{n}Pr (**5**), ^{n}Bu (**6**), CH_2SiMe_3 (**7**)] are all obtained by the reaction of **1** with the appropriate alkyl lithium or Grignard reagent (Scheme 4). Like complex **3**, the pyridine ring protons of complexes **4**−**7** can also be equilibrated at elevated temperatures, consistent with a ring-rocking process occurring in these species as well. At 25 °C, the approximate energy for this exchange process increases in the order **4** (16.5 ± 0.2 kcal mol^{-1}) < **5** (17.1 ± 0.2 kcal mol^{-1}) < **6** (17.6 ± 0.2 kcal mol^{-1}) < **7** (>19 kcal mol^{-1}). However, despite the presence of β-hydrogens in complexes **4**−**6**, these derivatives appear stable toward β-hydrogen elimination. (Other Ta(III) alkyls such as $(\eta^6$-$C_6Me_6)Ta(OAr)Et_2$ have also been reported

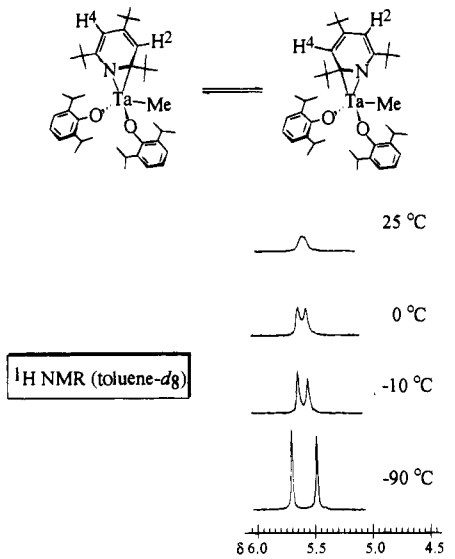

Figure 3. Partial ^{1}H NMR spectrum of $[\eta^2(N,C)$-2,4,6-$NC_5{}^tBu_3H_2]$-$Ta(OAr)_2Me$ (**3**) indicating the resonances of the pyridine ring protons. Spectra were recorded in toluene-d_8.

Scheme 5

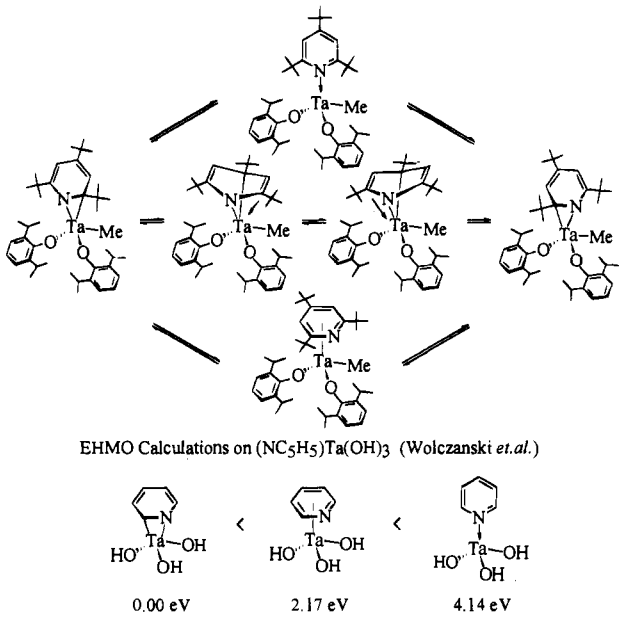

to exhibit marked stability toward a β-H elimination process.[50] Complexes **4**−**6**, nevertheless, represent the kinetic products of the reaction as they all undergo thermolytic decomposition (*vide infra*) in a process that does not involve β-hydrogen elimination.

The reaction of $[\eta^2(N,C)$-2,4,6-$NC_5{}^tBu_3H_2]Ta(OAr)_2Cl$ (**1**) with 1 equiv of ^{t}BuLi (benzene/pentane, room temperature, 2 h) takes a different course; the major product obtained in this reaction is the ring-opened compound Ta(=NC^{t}Bu=CHC^{t}Bu=CHCH^{t}Bu)$(OAr)_2$ (**2**) (Scheme 6). Whether a discrete *tert*-butyl intermediate is formed that subsequently β-H eliminates (as depicted in Scheme 6) or whether delivery of H$^-$ directly to the metal from ^{t}BuLi occurs is inconsequential; the results described for the other carbon nucleophiles decisively advance the *metal* as the site of nucleophilic attack in this reaction and therefore an intermediate hydride complex is strongly implicated.

(50) Arney, D. J.; Bruck, M. A.; Wigley, D. E. *Organometallics* **1991**, *10*, 3947.

Scheme 6

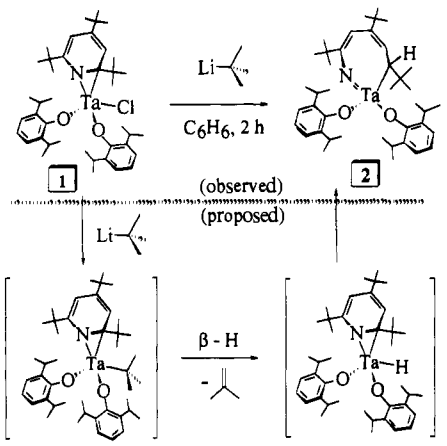

Scheme 7

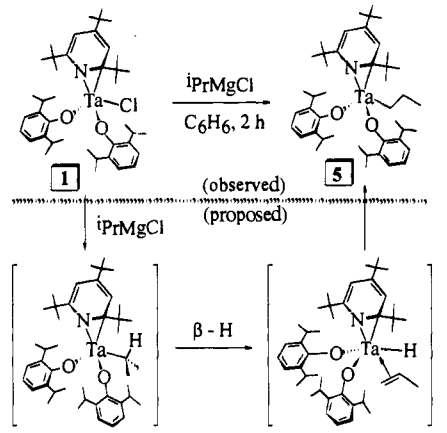

The reaction of **1** with ^{t}BuLi affords **2** as the major product even when this reaction is run in the presence of excess CH_2=$CHCMe_3$ or excess CH_2=CH_2, or in *neat* CH_2=$CHCMe_3$; no evidence for trapping an intermediate hydride complex with these reagents is observed.

The reaction of $[\eta^2(N,C)$-2,4,6-$NC_5{}^tBu_3H_2]Ta(OAr)_2Cl$ (**1**) with 1 equiv of ^{i}PrMgCl in (benzene/THF, room temperature, 2 h) is also instructive. Under these conditions, the major product is the *n-propyl* derivative $[\eta^2(N,C)$-2,4,6-$NC_5{}^tBu_3H_2]Ta(OAr)_2(^n$Pr) (**5**). Rapid workup of this reaction (ca. 15 min) allows the observation of small concentrations of a compound formulated as the isopropyl derivative, but **5** increases in concentration at the expense of this product over time. This reaction is proposed to involve rearrangement by β-H elimination and an intermediate hydride propene complex as shown in Scheme 7. Isomerization does not appear to involve complete CH_2=CHMe dissociation from the intermediate propene hydride complex, since reacting **1** with ^{i}PrMgCl in the presence of excess CH_2=$CHCMe_3$ affords *only* $[\eta^2(N,C)$-2,4,6-$NC_5{}^tBu_3H_2]$-$Ta(OAr)_2(^n$Pr) (**5**); no evidence for trapping a hydride complex is obtained.

The differences in steric requirements of tertiary *vs* secondary *vs* primary alkyl derivatives $[\eta^2(N,C)$-2,4,6-$NC_5{}^tBu_3H_2]Ta(OAr)_2R$ appear sufficient to account for these observations. For the *tert*-butyl complex, β-H elimination generates bulky CH_2=CMe_2 and therefore olefin loss without reinsertion is facile; hydride migration from incipient $[\eta^2(N,C)$-2,4,6-$NC_5{}^tBu_3H_2]$-$Ta(OAr)_2(H)$ subsequently occurs. In the isopropyl derivative, β-H elimination and CH_2=CHMe reinsertion (and isomerization) are faster than either olefin loss *or hydride migration* and allow the stable primary alkyl complex **5** to form. As long as steric constraints are not severe, as in the primary alkyl compounds **3**–**6**, the ground state is sufficiently stable that β-H elimination is no longer facile and other reaction pathways ensue upon thermolysis before β-H elimination can begin (*vide infra*).

Table 3. Selected Bond Distances (Å) and Bond Angles (deg) in $[\eta^2(N,C)$-2,4,6-$NC_5{}^tBu_3H_2]Ta(OAr)_2Et$ (**4**)[a]

	Bond Distances		
Ta–N	1.971(6)	C(2)–C(3)	1.35(1)
Ta–C(1)	2.152(7)	C(3)–C(4)	1.44(1)
Ta–C(7)	2.20(1)	C(4)–C(5)	1.37(1)
Ta–O(10)	1.884(5)	C(5)–N	1.42(1)
Ta–O(20)	1.898(5)	O(10)–C(11)	1.377(9)
N–C(1)	1.467(9)	O(20)–C(21)	1.387(9)
C(1)–C(2)	1.48(1)		
	Bond Angles[b]		
C(7)–Ta–O(10)	101.0(4)	C(1)–C(2)–C(3)	121.7(8)
C(7)–Ta–O(20)	104.7(4)	C(2)–C(3)–C(4)	118.9(8)
C(7)–Ta–N,C	110.0(3)[c]	C(3)–C(4)–C(5)	122.3(9)
O(10)–Ta–O(20)	105.6(2)	C(4)–C(5)–N	115.7(9)
O(10)–Ta–N,C	116.9(1)[c]	Ta–C(7)–C(8)	127.(1)
O(20)–Ta–N,C	116.9(1)[c]	Ta–O(10)–C(11)	158.5(5)
Ta–N–C(5)	141.7(6)	Ta–O(20)–C(21)	149.7(5)
Ta–C(1)–C(2)	112.3(5)		

[a] Numbers in parentheses are estimated standard deviations in the least significant digits. [b] The designation "N,C" represents the midpoint of the N–C(1) bond. [c] This value was generated without the covariance matrix therefore the esd was obtained using the standard *x*, *y*, and *z* esd's from atomic parameters.

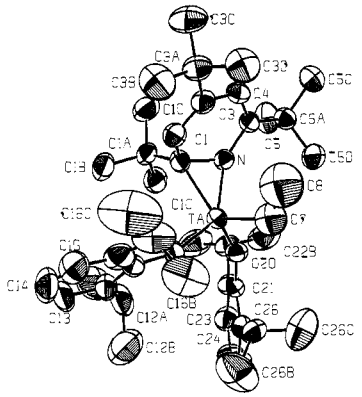

Figure 4. Molecular structure of $[\eta^2(N,C)$-2,4,6-$NC_5{}^tBu_3H_2]Ta(OAr)_2$-Et (**4**) with atoms represented as 50% ellipsoids.

Structural Study of $[\eta^2(N,C)$-2,4,6-$NC_5{}^tBu_3H_2]Ta(OAr)_2Et$ (4). Orange, single crystals of **4** suitable for an X-ray structural determination were grown from Et_2O/acetonitrile at −35 °C. Tables 1 and 3 present details of the structural study and selected structural data, respectively, and Figure 4 presents the molecular structure of **4**.

The molecular structure of **4** unambiguously establishes that ethyl addition has occurred at the metal center and that the $\eta^2(N,C)$-pyridine ligand is relatively unaffected by its presence. The tantalum pyridine interaction in **4** features a Ta–N bond of 1.971(6) Å and a Ta–C(1) distance of 2.152(7) Å, similar to the structure of **1**. The N–C(1) distance of 1.467(9) Å supports the description of **4** as a Ta(V)-metallaaziridine species[41–44] rather than an η^2-imine complex of Ta(III). No other close approaches of the remaining atoms of the pyridine ligand are evident. The angle between the best pyridine plane and the Ta–N–C(1) plane is 120.53 ± 0.27°. Additionally, a 1,3-diene type π electron localization is readily apparent in the η^2 pyridine ligand of **4** as the C(2)–C(3) and C(4)–C(5) bonds average 1.36(1) Å while the C(1)–C(2) and C(3)–C(4) bonds average 1.46(2) Å. An interruption of aromaticity of this same type has been noted in the structures of $[\eta^2(N,C)$-$NC_5H_5]Ta(OSi^tBu_3)_3$[45,46] and the 6-methylquinoline derivatives $[\eta^2(N,C)$-$NC_{10}H_9]Ta(OAr)_3(PMe_3)$ and $[\eta^2(N,C)$-$NC_{10}H_9]$-

Scheme 8

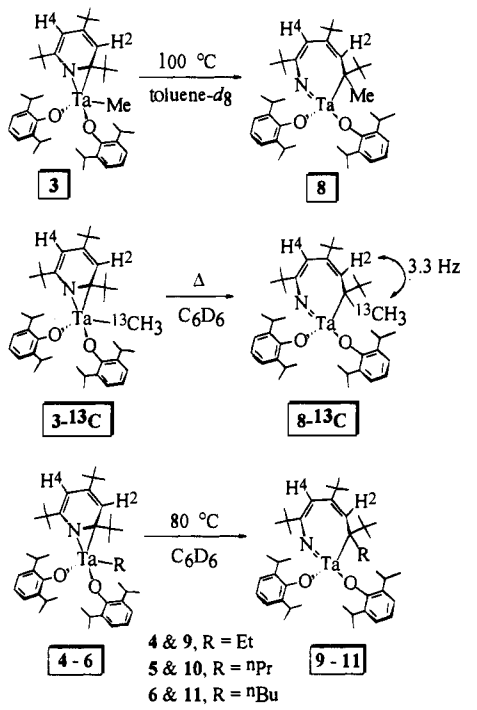

$Ta(OAr)_2Cl(OEt_2)$.[51,52] A comparison of the geometries of $[\eta^2(N,C)$-2,4,6-$NC_5{}^tBu_3H_2]Ta(OAr)_2Et$ (**4**) and $[\eta^2(N,C)$-2,4,6-$NC_5{}^tBu_3H_2]Ta(OAr)_2Cl$ (**1**)[40] suggests that little overall change in the pyridine ligand is exhibited upon complex alkylation, although the relative orientation of the pyridine ligand with respect to the Cl or Et substituent in the $Ta(OAr)_2X$ core is different. Thus, the chloride substituent is *cis* to C(1) in **1** while the ethyl substituent is *cis* to N in **4**.

Decomposition of $[\eta^2(N,C)$-2,4,6-$NC_5{}^tBu_3H_2]Ta(OAr)_2$-Me: Transition-Metal-Mediated C−N Bond Cleavage. While carbon nucleophiles are observed to attack the metal center in $[\eta^2(N,C)$-2,4,6-$NC_5{}^tBu_3H_2]Ta(OAr)_2Cl$ (**1**) to afford complexes **3**−**7**, we have discovered that compounds **3**−**6** constitute the *kinetic* products of this system. Upon thermolyzing benzene solutions of **3** (80 °C, C_6D_6), a gradual darkening of the solution is observed, and after 36 h, the concentration of **3** has significantly diminished and a new complex **8** is observed. The ^{1}H NMR signals for H(2) and H(4) of the $\eta^2(N,C)$-2,4,6-$NC_5{}^tBu_3H_2$ ligand that are equivalent on the NMR time scale in **3** are replaced by two new, sharp singlets at δ 6.36 and 6.05 (C_6D_6) in **8** that cannot be rendered equivalent even at higher temperatures (100 °C, toluene-d_8). Based on the similarity of the NMR data of **8** to $Ta(=NC^tBu{=}CHC^tBu{=}CHCH^tBu)(OAr)_2$ (**2**), this new product is formulated as the C−N bond cleavage isomer, $Ta(=NC^tBu{=}CHC^tBu{=}CHC^tBuMe)(OAr)_2$ (**8**) (Scheme 8). The migration of the methyl group from metal to pyridine ligand is supported by the ^{1}H NMR spectrum of $Ta(=NC^tBu{=}CHC^tBu{=}CHC^tBu^{13}CH_3)(OAr)_2$ (**8**-^{13}***C***), {produced by thermolyzing $[\eta^2(N,C)$-2,4,6-$NC_5{}^tBu_3H_2]Ta(OAr)_2(^{13}CH_3)$ (**3**-^{13}***C***)} where the H(2) proton appears as a δ 6.36 doublet ($^3J_{CH}$ = 3.3 Hz) from coupling with the methyl ^{13}C nucleus (Scheme 8). The resonance assigned as the migrated methyl group (δ 3.17, singlet) in the ^{1}H NMR spectrum of **8** is shifted considerably downfield from its δ 1.17 location in **3**, an assignment that is confirmed by its absence in the deuterium-labeled derivative $Ta(=NC^tBu{=}CHC^tBu{=}CHC^tBuCD_3)(OAr)_2$ (**8**-***d*$_3$), formed upon thermolyzing $[\eta^2(N,C)$-2,4,6-$NC_5{}^tBu_3H_2]$-$Ta(OAr)_2(CD_3)$ (**3**-***d*$_3$).

All attempts to isolate pure $Ta(=NC^tBu{=}CHC^tBu{=}CHC^tBuMe)(OAr)_2$ (**8**) have been unsuccessful since **8** itself is unstable under the conditions required for its generation (*vide infra*). Therefore **8** has been generated neither in pure form nor in high concentrations, nor can it be selectively crystallized from the reaction solution. The other alkyl derivatives, $[\eta^2(N,C)$-2,4,6-$NC_5{}^tBu_3H_2]Ta(OAr)_2R$ [R = Et (**4**), ^{n}Pr (**5**), ^{n}Bu (**6**)], also decompose under similar conditions (80 °C, C_6D_6) to afford the C−N bond scission products $Ta(=NC^tBu{=}CHC^tBu{=}CHC^tBuR)(OAr)_2$ [R = Et (**9**), ^{n}Pr (**10**), ^{n}Bu (**11**)] (Scheme 8); partial ^{1}H NMR data for complexes **8**−**11** are compiled in Table 4. The α-methylene protons of the migrated alkyl groups become diastereotopic β-hydrogens in **9**−**11** and appear as well-separated multiplets at ca. δ 4.4 and 3.0. As in complex **8**, the thermal instability of **9**−**11** has also precluded their isolation. Under conditions that induce alkyl migration in **3**−**6**, the $-CH_2SiMe_3$ complex $[\eta^2(N,C)$-2,4,6-$NC_5{}^tBu_3H_2]Ta(OAr)_2$-$(CH_2SiMe_3)$ (**7**) is stable. Thus, thermolyzing **7** for days (C_6D_6, 100 °C, sealed tube) results in no decomposition, perhaps reflecting the steric limitations of the alkyl migration.

Mechanistic Studies of the Metal-to-Ligand Alkyl Migration in the Conversion of $[\eta^2(N,C)$-2,4,6-$NC_5{}^tBu_3H_2]Ta$-$(OAr)_2Me$ to $Ta(=NC^tBu{=}CHC^tBu{=}CHC^tBuMe)(OAr)_2$. Determining whether the $[\eta^2(N,C)$-2,4,6-$NC_5{}^tBu_3H_2]Ta(OAr)_2$-Me (**3**) → $Ta(=NC^tBu{=}CHC^tBu{=}CHC^tBuMe)(OAr)_2$ (**8**) conversion occurs in an *intra*- or *inter*molecular fashion is central to understanding the role of the transition metal in mediating C−N bond cleavage and therefore in addressing a fundamental question surrounding HDN catalysis. To examine this process, a simple crossover experiment was carried out which takes advantage of the three-bond $^3J_{CH}$ coupling observed for the H(2) proton in the ^{1}H NMR spectrum of $Ta(=NC^tBu{=}CHC^tBu{=}CHC^tBu^{13}CH_3)(OAr)_2$ (**8**-^{13}***C***) (Scheme 8). Thus, an equimolar mixture of $[\eta^2(N,C)$-2,4,6-$NC_5{}^tBu_3D_2]Ta(OAr)_2Me$ (**3**-***d*$_2$) and $[\eta^2(N,C)$-2,4,6-$NC_5{}^tBu_3H_2]Ta(OAr)_2(^{13}CH_3)$ (**3**-^{13}***C***) was thermolyzed (C_6D_6 sealed tube, 120 °C, 4 h) and the resulting ring cleaved products observed by ^{1}H NMR (Scheme 9). The H(2) resonance of the cleavage product appeared as a doublet *only* in the ^{1}H NMR spectrum of this reaction, implying that *only* $Ta(=NC^tBu{=}CDC^tBu{=}CDC^tBuMe)(OAr)_2$ (**8**-***d*$_2$) and $Ta(=NC^tBu{=}CHC^tBu{=}CHC^tBu^{13}CH_3)(OAr)_2$ (**8**-^{13}***C***) were

Table 4. Partial ^{1}H NMR Data (C_6D_6) for Metallacyclic Imido Complexes $Ta(=NC^tBu{=}CHC^tBu{=}CHC^tBuR)(OAr)_2$ Derived from Metal-to-Ligand Alkyl Migration[a,b]

complex	H(2)	H(4)	$CHMe_2$ (OAr)	CH_aH_bR'	CH_aH_bR
R = Me (**8**)	6.36 (br s)	6.05 (s)	3.95 and 3.75 (spt)	3.17 (s)	
R = Et (**9**)	6.23 (br s)	6.09 (s)	3.96 and 3.74 (spt)	4.46 (m)	3.04 (m)
R = ^{n}Pr (**10**)	6.22 (br s)	6.09 (s)	3.96 and 3.74 (spt)	4.38 (m)	2.90 (m)
R = ^{n}Bu (**11**)	6.23 (br s)	6.05 (s)	3.94 and 3.76 (spt)	4.42 (m)	2.98 (m)

[a] Chemical shifts in ppm in C_6D_6. [b] Ring numbering scheme: $Ta(=NC^tBu{=}CH^4C^tBu{=}CH^2C^tBuCH_aH_bR')(OAr)_2$.

(51) Allen, K. D.; Bruck, M. A.; Gray, S. D.; Kingsborough, R. P.; Smith, D. P.; Weller, K. J.; Wigley, D. E. *Polyhedron* **1995**, in press.

(52) The structures of the $\eta^2(N,C)$-6-methylquinoline complexes indicate a disruption of heterocyclic aromaticity *only*, while the carbocyclic ring is relatively unperturbed, consistent with selective heterocyclic hydrogenation under mild conditions (125 psi H_2). Refer to ref 51.

Scheme 9

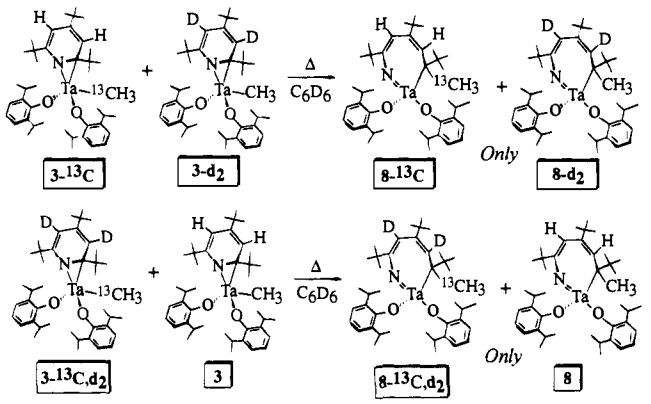

present in the sample; *none* of the possible crossover products Ta(=NC^{t}Bu=CHC^{t}Bu=CHC^{t}BuMe)(OAr)$_2$ (**8**) or Ta(=NC^{t}Bu=CDC^{t}Bu=CDC^{t}Bu^{13}CH$_3$)(OAr)$_2$ (**8-^{13}C,d$_2$**) was detected. Similarly, thermolyzing an equimolar mixture of [$\eta^2(N,C)$-2,4,6-NC$_5$^{t}Bu$_3$H$_2$]Ta(OAr)$_2$Me (**3**) and [$\eta^2(N,C)$-2,4,6-NC$_5$^{t}Bu$_3$-D$_2$]Ta(OAr)$_2$(^{13}CH$_3$) (**3-^{13}C,d$_2$**) in the reverse crossover experiment afforded *only* Ta(=NC^{t}Bu=CHC^{t}Bu=CHC^{t}BuMe)(OAr)$_2$ (**8**) and Ta(=NC^{t}Bu=CDC^{t}Bu=CDC^{t}Bu^{13}CH$_3$)(OAr)$_2$ (**8-^{13}C,d$_2$**) (Scheme 9). The results of these experiments unambiguously demonstrate that methyl migration in the **3** → **8** reaction occurs in an *intramolecular* fashion.

Kinetic studies of the conversion of [$\eta^2(N,C)$-2,4,6-NC$_5$^{t}Bu$_3$H$_2$]Ta(OAr)$_2$Me (**3**) to Ta(=NC^{t}Bu=CHC^{t}Bu=CHC^{t}BuMe)(OAr)$_2$ (**8**) by ^{1}H NMR (toluene-d_8, 100 °C) revealed that the disappearance of **3** obeys first-order kinetics (R^2 = 0.981) over greater than 3 half-lives, consistent with the crossover experiments. The reaction is quite slow at this temperature ($t_{1/2}$ = 8.75 h) and the C−N bond cleavage product **8** reaches a steady state concentration after approximately 1 half-life owing to its decomposition under these conditions. Preliminary rate studies (C_6D_6, 80 °C) of the decomposition of **4**−**6** indicate that the rate of metal → ligand alkyl migration for [$\eta^2(N,C)$-2,4,6-NC$_5$^{t}Bu$_3$H$_2$]Ta(OAr)$_2$R decreases in the following order: R = Et > ^{n}Pr ~ ^{n}Bu ≫ Me.

Further Heterocycle Degradation in the Decomposition of the Ring-Opened Species Ta(=NC^{t}Bu=CHC^{t}Bu=CHC^{t}BuMe)(OAr)$_2$: Formation of a Metallapyridine Complex. While the alkyl complexes [$\eta^2(N,C)$-2,4,6-NC$_5$^{t}Bu$_3$H$_2$]Ta(OAr)$_2$R (**3**−**6**) have been shown to constitute kinetic products of this system, the ring-opened metallacycles Ta(=NC^{t}Bu=CHC^{t}Bu=CHC^{t}BuR)(OAr)$_2$ (**8**−**11**) have also been identified as unstable kinetic products. Upon exhaustive thermolysis of solutions of [$\eta^2(N,C)$-2,4,6-NC$_5$^{t}Bu$_3$H$_2$]Ta(OAr)$_2$Me (**3**, 140 °C, 10 days), the first formed metallacycle Ta(=NC^{t}Bu=CHC^{t}Bu=CHC^{t}BuMe)(OAr)$_2$ (**8**) undergoes further decomposition to afford a quantitative yield of orange, air- and moisture-stable **13**. This species is completely insoluble in common organic solvents as well as dilute aqueous solutions of HF, therefore spectroscopic characterization has been precluded. However, it was possible to grow X-ray quality crystals directly from the decomposition of **3** in hot benzene (sealed tube, 110 °C). The X-ray structural study (*vide infra*) of this robust molecule reveals it to be a dimer of the formal metallapyridine complex, [Ta(μ-NC^{t}Bu=CHC^{t}Bu=CH)(OAr)$_2$]$_2$ (**13**) (Figure 5 and Scheme 10). This section will address the mechanistic questions of this conversion, while the structural results are described below.

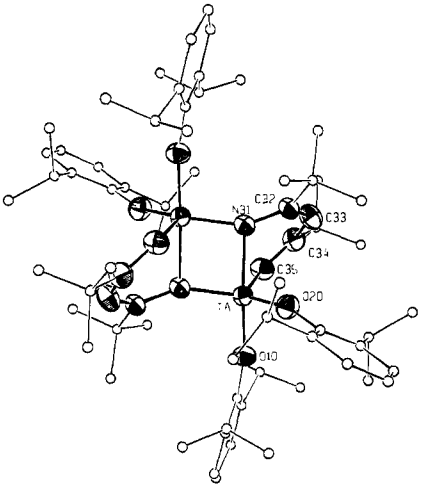

Figure 5. Molecular structure of [Ta(μ-NC^{t}Bu=CHC^{t}Bu=CH)(OAr)$_2$]$_2$ (**13**) with local atoms represented as 50% ellipsoids.

Scheme 10

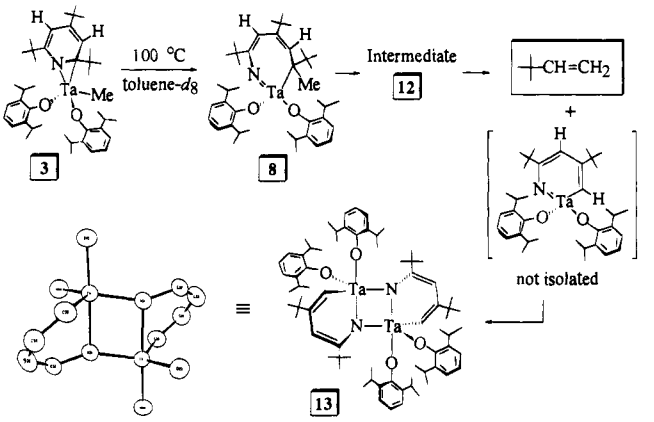

In the **3** → **8** → **13** conversion, the net loss of 1 equiv of *tert*-butylethylene per tantalum has apparently occurred, and indeed monitoring the reaction in a sealed NMR tube (C_6D_6, 110 °C) reveals that 0.91 equiv of ^{t}BuCH=CH$_2$ [(Me$_3$Si)$_2$O internal standard] is formed per equiv of **3** consumed. In order to establish the origin of the *tert*-butylethylene and more firmly understand the mechanism of this rearrangement, the results of the following labeling studies are reported (Scheme 11).

(i) Thermolysis of [$\eta^2(N,C)$-2,4,6-NC$_5$^{t}Bu$_3$D$_2$]Ta(OAr)$_2$Me (**3-d$_2$**) provides Ta(=NC^{t}Bu=CDC^{t}Bu=CDC^{t}BuMe)(OAr)$_2$ (**8-d$_2$**) that further degrades to form *only* ^{t}BuCH=CH$_2$. No deuterium incorporation in the resulting olefin is observed.

(ii) Thermolysis of [$\eta^2(N,C)$-2,4,6-NC$_5$^{t}Bu$_3$H$_2$]Ta(OAr)$_2$(CD$_3$) (**3-d$_3$**) produces Ta(=NC^{t}Bu=CHC^{t}Bu=CHC^{t}BuCD$_3$)(OAr)$_2$ (**8-d$_3$**) that upon further degradation affords *only* ^{t}BuCD=CD$_2$.

(iii) Upon thermolysis of [$\eta^2(N,C)$-2,4,6-NC$_5$^{t}Bu$_3$-H$_2$]Ta(OAr)$_2$(^{13}CH$_3$) (**3-^{13}C**), *only* ^{t}BuCH=^{13}CH$_2$ is formed via intermediate Ta(=NC^{t}Bu=CHC^{t}Bu=CHC^{t}Bu^{13}CH$_3$)(OAr)$_2$ (**8-^{13}C**).

The deuterium labeling results i and ii clearly indicate that the *migrating methyl group* in the **3** → **8** → **13** decomposition serves as the sole source for *all three* olefinic hydrogens of the *tert*-butylethylene produced. Additionally, the ^{13}C-labeling

Scheme 11

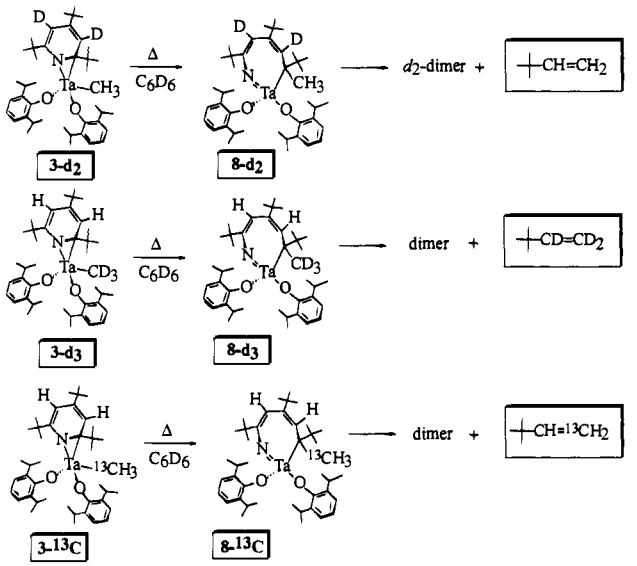

experiment iii demonstrates that the methyl group of **3** (and **8**) serves as the sole source of the terminal, methylene carbon of the resulting ^{t}BuCH=CH$_2$.

While the source of the *tert*-butylethylene has been identified, the mechanism of its formation has not. Fortunately this **8** → **13** decomposition is accompanied by the formation of a small concentration, and then smooth disappearance, of a species that constitutes *another* intermediate in the reaction, complex **12**. Therefore the sequence of *observed* compounds for pyridine ring cleavage and degradation is proposed to be **3** → **8** → **12** → **13**. The ^{1}H NMR data for **12** reveal that (i) ^{t}BuCH=CH$_2$ has not been lost from this complex, (ii) the former ^{1}H resonance for the β-methyl group of **8** has been transformed into an AMX set of mutiplets in the aliphatic region of **12** (δ 2.93, 2.50, and 1.90; 1 H each), and (iii) the H(2) singlet in the ^{1}H NMR spectrum of **8** now appears as a δ 5.50 *doublet* coupled to the δ 2.93 multiplet of the ABX set. The most consistent explanation for these data is that the AMX multiplets arise from protons attached to the α and β carbons in a new complex with the connectivity TaC_αH$_2$C$_\beta$H^{t}Bu. Therefore complex **12** is formulated as the *eight-membered*, metallacyclic species Ta(=NC^{t}Bu=CHC^{t}Bu=CHC^{t}BuHCH$_2$)(OAr)$_2$ shown in Figure 6.

An adduct of **12** can be *isolated* upon performing the decomposition of [η^2(*N,C*)-2,4,6-NC$_5{}^t$Bu$_3$H$_2$]Ta(OAr)$_2$Me (**3**) in the presence of a coordinating ligand. Thus, heating benzene solutions (100 °C, 3 days) of **3** in the presence of excess PMe$_3$, followed by crystallization from acetonitrile/Et$_2$O solutions, provides colorless crystals of Ta(=NC^{t}Bu=CHC^{t}Bu=CHC^{t}BuHCH$_2$)(OAr)$_2$·2NCMe (**12-NCMe**) in which any PMe$_3$ which may have been coordinated has been displaced by NCMe (Scheme 12 and Figure 7). The ^{1}H NMR data of this complex reveal the same AMX set of multiplets in the aliphatic region (at δ 2.96, 2.35, and 1.76; 1 H each) with the resonance associated with the former H(2) hydrogen of **8** appearing as a δ 5.49 doublet coupled to the δ 2.96 resonance. Analytical and spectroscopic data for Ta(=NC^{t}Bu=CHC^{t}Bu=CHC^{t}BuHCH$_2$)(OAr)$_2$·2NCMe (**12-NCMe**) suggest that under prolonged vacuum **12-NCMe** slowly loses NCMe, thus Ta(=NC^{t}Bu=CHC^{t}Bu=CHC^{t}BuHCH$_2$)(OAr)$_2$·2NCMe is considered the maximum NCMe incorporation in this complex. The elemental analysis of **12-NCMe** predicts 1.6−1.7 acetonitrile molecules per tantalum, thus it is possible that only one NCMe is coordinated in this complex and a lattice NCMe is more susceptible to loss under vacuum. Unfortunately, crystallographic quality samples of **12-NCMe** have not yet been obtained.

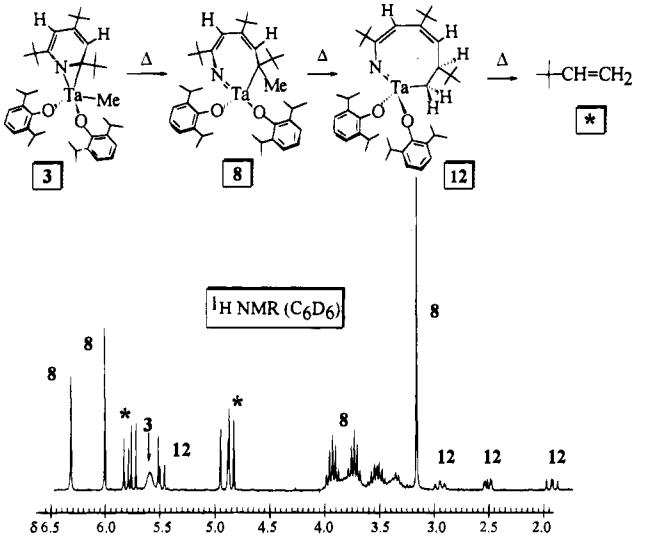

Figure 6. Partial ^{1}H NMR spectrum (C_6D_6) of the solution formed upon thermolysis of [η^2(*N,C*)-2,4,6-NC$_5{}^t$Bu$_3$H$_2$]Ta(OAr)$_2$Me (**3**). Resonances associated with Ta(=NC^{t}Bu=CHC^{t}Bu=CHC^{t}BuCH$_3$)(OAr)$_2$ (**8**), Ta(=NC^{t}Bu=CHC^{t}Bu=CHC^{t}BuHCH$_2$)(OAr)$_2$ (**12**), and ^{t}BuCH=CH$_2$ (*) are indicated.

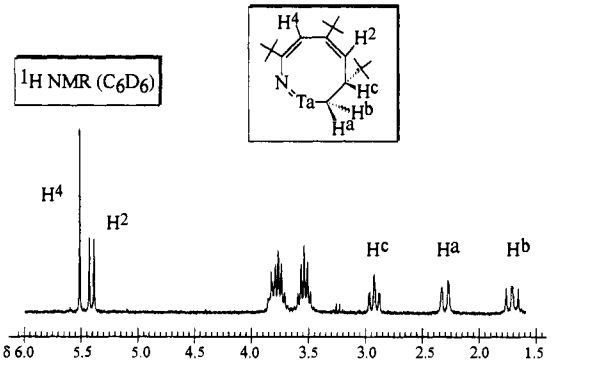

Figure 7. Partial ^{1}H NMR spectrum (C_6D_6) of Ta(=NC^{t}Bu=CHC^{t}Bu=CHC^{t}BuHCH$_2$)(OAr)$_2$·2NCMe (**12-NCMe**) emphasizing the metallacyclic ^{1}H resonances.

Scheme 12

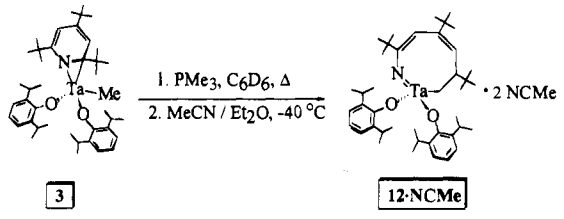

The eight-membered metallacycle Ta(=NC^{t}Bu=CHC^{t}Bu=CHC^{t}BuHCH$_2$)(OAr)$_2$ (**12**) can be considered as a "ring expansion" product arising from the seven-membered metallacycle **8**. The formulation of **12** is further supported by the following experiments.

Scheme 13

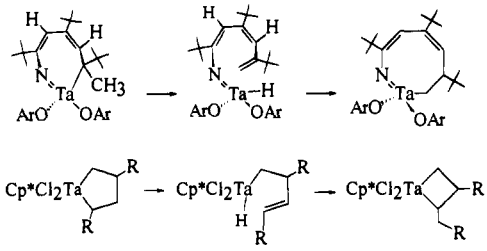

Scheme 14

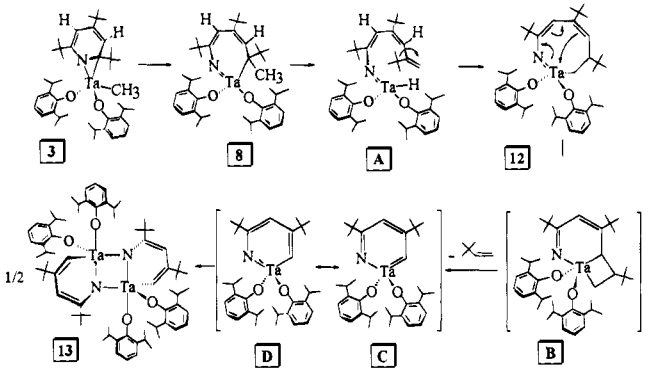

(i) Upon thermolysis of the deuterium-labeled derivative Ta(=NᵗBu=CHᵗBu=CHᵗBuCD₃)(OAr)₂ (**8-*d*₃**, produced in the thermolysis of **3-*d*₃**), the AMX aliphatic signals of **12-*d*₃** (labeled as **12** between δ 3.0 and 2.8, Figure 6) are absent and the resonance assigned to ring hydrogen H(2) (δ 5.5, Figure 6) appears as a broad singlet. Complex **12-*d*₃** is therefore formulated as Ta(=NᵗBu=CHᵗBu=CHᵗBuDCD₂)(OAr)₂. This observation reveals that the protons of the migrated methyl group of **8** are incorporated *exclusively* into the α- and β-positions of the ring expansion product **12**.

(ii) Upon thermolyzing the ^{13}C-labeled complex Ta(=NᵗBu=CHᵗBu=CHᵗBu^{13}CH₃)(OAr)₂ (**8-^{13}*C***, produced in the thermolysis of **3-^{13}*C***), the AMX aliphatic signals of **12-^{13}*C*** are all further split into complex multiplets in its ^{1}H NMR spectrum. Therefore, complex **12-^{13}*C*** is formulated as Ta(=NᵗBu=CHᵗBu=CHᵗBuH^{13}CH₂)(OAr)₂.

An analogy between the classic "ring contraction" reaction, established in tantalacyclo*pentane* → tantalacyclo*butane* rearrangements and our formal "ring expansion" process may be drawn to provide a reasonable mechanism of the **8** → **12** conversion (Scheme 13). Therefore, we propose that a simple β-hydrogen elimination to provide transient Ta(=NᵗBu=CHᵗBu=CHᵗBu=CH₂)(H)(OAr)₂ (**A**) occurs and that **A** subsequently undergoes rapid olefin reinsertion in the opposite sense to afford Ta(=NᵗBu=CHᵗBu=CHᵗBuHCH₂)(OAr)₂ (**12**) (Scheme 13). Both Schrock's ring contraction rearrangement and this formal ring expansion appear to initiate by β-hydrogen elimination, and in both systems, the resulting d^0 tantalum hydrides cannot bind the olefin strongly which allows for facile C−C bond rotation and reinsertion as shown. The observation that Ta(=NᵗBu=CHᵗBu=CHCHᵗBu)(OAr)₂ (**2**) and Ta(=NᵗBu=CHᵗBu=CHᵗBuPh)(OAr)₂[53] —which contain *no* β-hydrogens—are indefinitely stable at elevated temperatures is consistent with the proposal that the decomposition of **8** involves an initial β elimination as proposed in Scheme 13.

Although no additional intermediates in the Ta(=NᵗBu=CHᵗBu=CHᵗBuHCH₂)(OAr)₂ (**12**) → ½[Ta(μ-NᵗBu=CHᵗBu=CH)(OAr)₂]₂ (**13**) + ᵗBuCH=CH₂ reaction have been detected, we can suggest a mechanistic scheme to account for this rearrangement (Scheme 14). Thus, electrocyclic rearrangement of the eight-membered metallacycle **12** to the substituted bicyclic complex **B** (Scheme 14), analogous to the reversible, disrotatory cyclization of 1,3,5-cyclooctatriene to provide bicyclo[4.2.0]octa-2,4-diene, eq 1, is proposed. A

(1)

1,3,5-cyclooctatriene — bicyclo[4.2.0]octa-2,4-diene

subsequent retro [2 + 2] cycloaddition of the metallacyclobutane portion of the bicyclic intermediate would provide the monomeric metallapyridine **C** and ᵗBuCH=CH₂. We represent metallapyridine **C** [Ta(=CHᵗBu=CHᵗBu=N)(OAr)₂] as π localized in the alkylidene form and suggest the observed π localized structure of the dimeric [Ta(μ-NᵗBu=CHᵗBu=CH)(OAr)₂]₂ (**13**, *vide infra*) may reflect a **C** → **D** electrocyclic process that regenerates a strong Ta=NR imido bond in metallapyridine **D** [Ta(=NᵗBu=CHᵗBu=CH)(OAr)₂] (Scheme 14). Putative metallapyridine **D** is proposed to rapidly dimerize to **13**. The strong imido Ta=NR bond in metallapyridine **D** and the insolubility and stability of **13** represent sizable driving forces for this rearrangement that force the ring degradation process to completion. We note, however, that a direct **12** → **D** + ᵗBuCH=CH₂ conversion may also be effected by a β-alkyl elimination from complex **12**,[54,55] a process that would maintain the strong Ta=N multiple bond throughout and circumvent putative intermediates **B** and **C**.

Further Heterocycle Degradation of Ta(=NᵗBu=CHᵗBu=CHᵗBuR)(OAr)₂ for R = Et, ⁿPr, or ⁿBu. The other C−N bond cleavage products Ta(=NᵗBu=CHᵗBu=CHᵗBuR)(OAr)₂ [R = Et (**9**), ⁿPr (**10**), ⁿBu (**11**)] reported above also decompose upon exhaustive thermolysis to form orange air- and moisture-stable crystalline solids, all with analytical data consistent for their formulation as the same metallapyridine [Ta(μ-NᵗBu=CHᵗBu=CH)(OAr)₂]₂ (**13**). Preliminary crystallographic analysis of the sample collected from thermolyzing Ta(=NᵗBu=CHᵗBu=CHᵗBuEt)(OAr)₂ (**9**) reveals identical unit cell dimensions as **13**, therefore we formulate this sample as the metallapyridine [Ta(μ-NᵗBu=CHᵗBu=CH)(OAr)₂]₂. In addition to the metallapyridine, complexes **9**−**11** also afford substituted *tert*-butylethylenes ᵗBuCH=CHR′ (by GC−mass spec) as the only other products from their decomposition. Thus, for Ta(=NᵗBu=CHᵗBu=CHᵗBuEt)(OAr)₂ (**9**), *cis*- and *trans*-ᵗBuCH=CHMe are identified; ther-

(53) Weller, K. J.; Gray, S. D.; Wigley, D. E. Unpublished results.

(54) Bunel, E.; Burger, B. J.; Bercaw, J. E. *J. Am. Chem. Soc.* **1988**, *110*, 976.

(55) McNeill, K.; Andersen, R. A.; Bergman, R. G. *J. Am. Chem. Soc.* **1995**, *117*, 3625.

Scheme 15

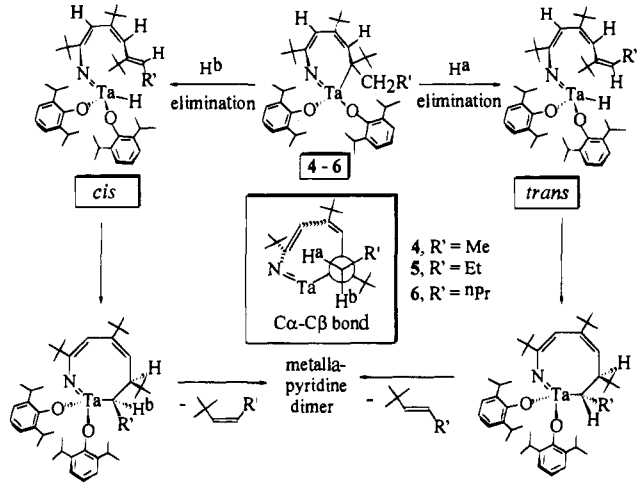

molyzing Ta(=NᵗBu=CHᵗBu=CHᵗBuⁿPr)(OAr)₂ (**10**) forms *cis*- and *trans*-ᵗBuCH=CHEt; and for Ta(=NᵗBu=CHᵗBu=CHᵗBuⁿBu)(OAr)₂ (**11**), *cis*- and *trans*-ᵗBuCH=CHⁿPr are produced. These results are consistent with the mechanism proposed in Scheme 14 for the ring degradation of Ta(=NᵗBu=CHᵗBu=CHᵗBuMe)(OAr)₂ (**8**) since these products constitute the *exact alkenes predicted by this mechanism* when **9**–**11** are decomposed.

An analogous mechanism for the decomposition of **9**–**11** to form **13** and ᵗBuCH=CHR′ is shown in Scheme 15. This proposal is supported by the labeling experiments used to develop Scheme 14 and provides a clear explanation for how both *cis*- and *trans*-ᵗBuCH=CHR′ arise. Since the complexes Ta(=NᵗBu=CHᵗBu=CHᵗBuR)(OAr)₂ **9**–**11** contain inequivalent, diasterotopic β-hydrogens, and since one of these β-hydrogens must nearly eclipse the metal center to undergo β-hydrogen elimination (viewed down the $C_\alpha-C_\beta$ bond), then both possible olefin stereochemistries may be obtained depending upon which β-hydrogen is eliminated (Scheme 15). The observed olefin stereochemistry in ᵗBuCH=CHR′ is therefore set at the β-H elimination step and *prior* to subsequent reinsertion and ring expansion as indicated in Scheme 15.

Structural Study of [Ta(μ-NᵗBu=CHᵗBu=CH)(OAr)₂]₂ (13). Orange to red, X-ray quality crystals of [Ta(μ-NᵗBu=CHᵗBu=CH)(OAr)₂]₂ (**13**) were grown directly from the decomposition of [η^2(*N*,*C*)-2,4,6-NC₅ᵗBu₃H₂]Ta(OAr)₂Me (**3**) in hot benzene (110 °C, sealed tube). Tables 1 and 5 present details of the structural study and selected bond lengths and angles, respectively, while Figure 5 presents a view of the centrosymmetric molecular structure of **13**.

The local coordination about each tantalum can be seen to be nearly trigonal bipyramidal with the fused TBP structures sharing an axial-equatorial edge. The two asymmetrically bridging nitrogen atoms of the [μ-NᵗBu=CHᵗBu=CH]$^{3-}$ ligands are formal bridging *imido* ligands that occupy the shared edge and display an equatorial Ta–N(31)* bond (1.906(3) Å) approximately 0.23 Å shorter than the axial Ta–N(31) bond (2.140(3) Å). By comparison, the asymmetric μ-tolylimido ligands in [Mo(=Ntol)(μ-Ntol)(OᵗBu)₂]₂ (also an edge-shared TBP structure) are much more asymmetric than those of **13** with equatorial Mo–N* bonds (1.842(7) Å) approximately 0.46 Å shorter than the axial Mo–N bonds (2.300(7) Å).[56-58] The significantly shorter equatorial Ta–N bond observed in **13** suggests a contribution of structures **E** and **F** to the complex with a minimum contribution of canonical form **G**.

Table 5. Selected Bond Distances (Å) and Bond Angles (deg) in [Ta(μ-NCᵗBu=CHCᵗBu=CH)(OAr)₂]₂ (**13**)[a,b]

Bond Distances			
Ta–N(31)	2.140(3)	C(34)–C(35)	1.343(6)
Ta–N(31)*	1.906(3)	Ta–O(10)	1.905(3)
Ta–C(35)	2.114(4)	Ta–O(20)	1.907(3)
N(31)–C(32)	1.409(5)	O(10)–C(11)	1.367(5)
C(32)–C(33)	1.352(6)	O(20)–C(21)	1.359(5)
C(33)–C(34)	1.454(7)		
Bond Angles			
N(31)–Ta–C(35)	82.8(2)	O(20)–Ta–N(31)*	127.4(1)
N(31)–Ta–N(31)*	82.6(1)	Ta–N(31)–C(32)	109.1(3)
N(31)–Ta–O(10)	176.3(1)	N(31)–C(32)–C(33)	120.8(4)
N(31)–Ta–O(20)	86.8(1)	C(32)–C(33)–C(34)	127.6(4)
C(35)–Ta–N(31)*	109.0(2)	C(33)–C(34)–C(35)	120.0(4)
C(35)–Ta–O(10)	93.9(1)	Ta–C(35)–C(34)	119.8(3)
C(35)–Ta–O(20)	120.5(2)	Ta–O(10)–C(11)	169.3(3)
O(10)–Ta–N(31)*	99.9(1)	Ta–O(20)–C(21)	160.5(3)
O(10)–Ta–O(20)	93.7(1)		

[a] Numbers in parentheses are estimated standard deviations in the least significant digits. [b] The atom N(31)* is related to N(31) by the crystallographic inversion center.

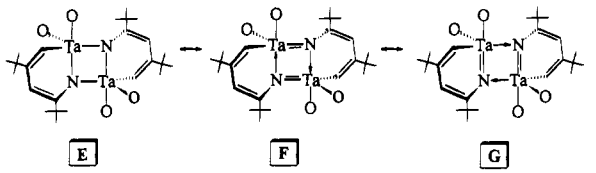

E F G

Another striking feature of the bridging metallacyclic [μ-NᵗBu=CHᵗBu=CH]$^{3-}$ ligand is its *localization* of the π electron density indicating that the "metallapyridine" manifests little aromaticity. This idea is further supported by the Ta–C(35) single bond of 2.114(4) Å indicating that the alkylidene structure Ta(=CHᵗBu=CHᵗBu=N)(OAr)₂ (**C**, Scheme 14) does not contribute significantly to the bonding. (Compare Ta–C(35) = 2.114(4) Å in **13** with the average Ta–C(sp²) bond distance of 2.104(8) Å in Ta(CᵗBu=CHCH=CᵗBu)(OAr)₂Cl.[40]) The comparatively close Ta···Ta separation of 3.0445(3) Å in this d^0–d^0 dimer further reflects the stability imparted through the μ-NR ligands. Space-filling models of **13** reveal the Ta_2N_2 core to be completely encapsulated in a hydrocarbon sheath which presumably accounts for the air and moisture stability of this complex.

Discussion

Despite its importance in producing high-quality, low-cost fuels and feedstocks, HDN catalysis is significantly less well-studied than HDS.[1-3] In particular, the elusive C–N bond scission step in HDN has necessarily been the subject of speculation rather than experimentation, since *no previous reactivity models of heterocycle C–N cleavage existed* prior to our report.[37] Therefore a critical examination of this model in view of proposed methods of C–N cleavage is instructive and

(56) Values for one independent molecule (of three) in the unit cell are reported here.

(57) Chisholm, M. H.; Folting, K.; Huffman, J. C.; Kirkpatrick, C. C.; Ratermann, A. L. *J. Am. Chem. Soc.* **1981**, *103*, 1305.

(58) Chisholm, M. H.; Folting, K.; Huffman, J. C.; Ratermann, A. L. *Inorg. Chem.* **1982**, *21*, 978.

Scheme 16

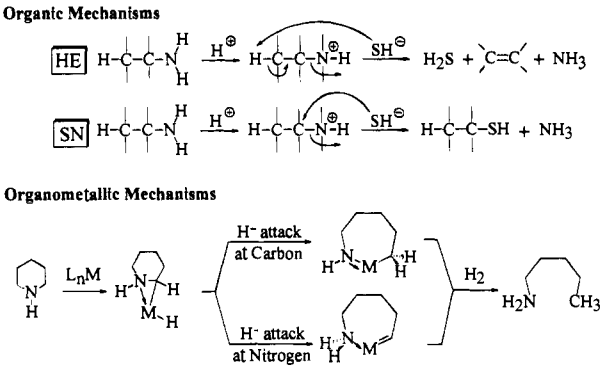

necessary for us to draw some conclusions regarding ways in which heterocyclic carbon−nitrogen bonds may be cleaved.

Quinoline is a prototypical HDN substrate which has proved particularly valuable in HDN model studies. It is generally believed (based primarily upon product ratios) that it is necessary to hydrogenate both the quinoline heterocycle and carbocycle ring in order to cleave both C−N bonds.[4,5,15−17,59] In a series of elegant kinetics studies, Satterfield and co-workers have established that H_2S that arises from HDS actually *enhances* the rate of quinoline HDN.[17−21] These observations, and related work from other groups,[16,59] have led many researchers to propose either a Hofmann elimination (HE), with SH^- serving as base, or a nucleophilic substitution (SN), with SH^- acting as nucleophile, as the principal mechanisms of C−N bond scission (Scheme 16).[4,5,7,8,22] In a recent mechanistic study, Perot and co-workers have obtained strong supporting evidence that the SN mechanism is the major HDN pathway in tetrahydro*isoquinoline* (THIQ).[22]

However, in many mechanistic discussions in the literature, the active participation of a metal center is not considered. Laine and co-workers have shown that no C−N bond cleavage in tertiary amines occurs up to 260 °C without the presence of a metal catalyst.[35,36] This study has led to the proposal that nucleophilic attack on a *coordinated* heterocycle is effecting the C−N bond scission in HDN chemistry.[7,8,14,60] Scheme 16 also outlines Laine's proposal for C−N bond scission in the saturated heterocycle piperidine.[7] A central feature of this proposal is the existence of an $\eta^2(N,C)$-*piperidyl* complex that is formed in a C−H activation step at the catalytic site. The subsequent C−N bond cleavage step involves hydride attack at either C_α, with the formation of an intermediate amido complex, or N, with the formation of an alkylidene. Laine's proposal is consistent with Satterfield's evidence that the H_2S rate enhancement effect occurs *in the C−N bond cleavage step*, rather than the hydrogenation steps,[21,61] further suggesting some type of nucleophilic attack of the heterocycle.

The C−N bond cleavage step we have observed with carbon nucleophiles (Scheme 8) shares three similarities with Laine's proposal. First, cleavage is found to occur only in an $\eta^2(N,C)$ complex. We have shown previously that the $\eta^2(N,C)$ bonding mode in complexes of quinoline also permits facile hydrogenation of the heterocycle (without reducing the carbocycle) and that $\eta^1(N)$ quinoline complexes are not readily reduced.[51] In this system, C−N bond scission has not been induced in d^0 or d^1 $\eta^1(N)$-pyridine or $\eta^1(N)$-quinoline complexes. Second, we have demonstrated that in the $\eta^2(N,C)$ mode, attack occurs at the pyridine *carbon*, rather than the nitrogen. In the metallaaziridine description of **1**, this reaction in our complexes transforms a formal *amido* nitrogen in the $\eta^2(N,C)$-pyridine to a formal *imido* nitrogen in the ring-opened structure in a reaction driven largely by the formation of a strong metal−ligand multiple bond. Laine's proposal differs from our observation in that under actual HDN conditions, the heterocyclic ring will be hydrogenated such that a formal *amine* nitrogen in the η^2-piperidyl ligand is converted to an *amido* nitrogen upon C−N bond cleavage. Third, C−N bond scission occurs via an *intra*molecular, *endo* attack of the migrating ligand. The results obtained for the carbon nucleophiles may also reflect the mechanism of C−N scission by hydride, since metal-mediated hydride attack on $\eta^2(N,C)$-heterocycles now appears to be a reasonable pathway.

Finally, this study offers new insight into how nitrogen heterocycles may be further degraded *after C−N bond cleavage* in HDN catalysis. An $\eta^2(N,C)$-pyridine ligand that ring opens in a manner so as to generate β hydrogens may be subject to further degradation as pathways exist for C−C bond cleavage by rearrangement of the ring-opened complex. Such information may be relevant to catalytic HDN since under normal HDN conditions ethane, ethene, propane, and propene are the principal products of pyridine HDN with only a minor fraction of C_5 products being generated.[39]

Conclusions

The results described in this report allow the following conclusions to be drawn and suggest the extent to which this system is a valid reactivity model for the active site in HDN catalysts.

(i) Structural and reactivity evidence point to a disruption of aromaticity of the heterocyclic ring in $\eta^2(N,C)$-pyridine compounds. Because the $\eta^2(C,C)$-pyridine or $\eta^2(C,C)$-quinoline coordination modes have not been observed in d^2 tantalum complexes, this interruption of aromaticity may accompany a *selective* activation of the heterocyclic C−N bond.

(ii) Carbon−nitrogen bond cleavage is found to occur only in the $\eta^2(N,C)$-pyridine complexes, and as indicated in our previous study, $\eta^2(N,C)$ coordination exists only in the d^2 oxidation state.[51] Given that the cobalt-promoter effect in MoS_2/γ-Al_2O_3 may include an electron transfer role,[62] our observations are perhaps relevant to changes in the substrate binding mode at the active site.

(iii) The $\eta^2(N,C)$ binding mode is observed to render the pyridine C_α susceptible to an apparent nucleophilic attack and this attack occurs invariably at the pyridine *carbon*, rather than nitrogen. Since imido ligands are apparently involved in other catalytic processes where the nitrogen is ultimately removed from the metal, (*e.g.* propylene ammoxidation,[63−68] and nitrile reduction[69−71]), the fact that the ring-opening reaction occurs with the formation of a tantalum imido ligand Ta=NR does not compromise the relevance of this model.

(59) Shih, S. S.; Katzer, J. R.; Kwart, H.; Stiles, A. B. *Am. Chem. Soc., Div. Pet. Chem. Prepr.* **1977**, *22*, 919.
(60) Shvo, Y.; Laine, R. M. *J. Chem. Soc., Chem. Commun.* **1980**, 753.
(61) Satterfield, C. N.; Carter, D. L. *Ind. Eng. Chem. Process Des. Dev.* **1981**, *20*, 538.
(62) Harris, S.; Chianelli, R. R. *J. Catal.* **1986**, *98*, 17.
(63) Grasselli, R. K.; Burrington, J. D. *Adv. Catal.* **1981**, *30*, 133.
(64) Burrington, J. D.; Katisek, C. T.; Grasselli, R. K. *J. Catal.* **1984**, *81*, 489 and references therein.
(65) Maatta, E. A.; Du, Y.; Rheingold, A. L. *J. Chem. Soc., Chem. Commun.* **1990**, 756.
(66) Maatta, E. A.; Du, Y. *J. Am. Chem. Soc.* **1988**, *110*, 8249.
(67) Chan, D. M.- T.; Fultz, W. C.; Nugent, W. A.; Roe, D. C.; Tulip, T. H. *J. Am. Chem. Soc.* **1985**, *107*, 251.
(68) Chan, D. M.-T.; Nugent, W. A. *Inorg. Chem.* **1985**, *24*, 1422.
(69) Bakir, M.; Fanwick, P. E.; Walton, R. A. *Inorg. Chem.* **1988**, *27*, 2016.
(70) Rhodes, L. F.; Venanzi, L. M. *Inorg. Chem.* **1987**, *26*, 2692.
(71) Han, S. H.; Geoffroy, G. L. *Polyhedron* **1988**, *7*, 2331.

(iv) The C−N bond scissions observed in these complexes occur *via* nucleophilic attack at the metal center first, followed by an *intra*molecular, *endo*-attack of the migrating ligand on the substrate. Therefore the same metal center in this model system is capable of activating the pyridine C−N bond and delivering the reagent (alkyl and perhaps hydride) that induces C−N bond scission.

(v) While there is no evidence that the Co−Mo−S or Ni−Mo−S phases in cobalt- or nickel-promoted MoS_2/γ-Al_2O_3 can induce C−N scission *prior* to heterocycle hydrogenation,[3] the reactions uncovered in this study offer the possibility that C−N bond cleavage may be promoted under milder conditions than are currently necessary. Whether the consumption of H_2 can be reduced by C−N scission *prior* to hydrogenation is not likely under existing hydrotreating conditions, since heterocycle hydrogenation (*e.g.* pyridine → piperidine or quinoline → 1,2,3,4-tetrahydroquinoline) is the most facile step in hydrotreating.

(vi) Carbon−carbon bond scissions of a ring-opened complex appear to be possible at the same metal site. Thus, in cases where a highly substituted metallacycle arises from pyridine ring-opening, further degradation pathways for C−C bond cleavage exist.

Experimental Section

General Details. All experiments were performed under a nitrogen atmosphere either by standard Schlenk techniques[72] or in a Vacuum Atmospheres HE-493 drybox at room temperature (unless otherwise indicated). Solvents were distilled under N_2 from an appropriate drying agent[73] and were transferred to the drybox without exposure to air. NMR solvents were passed down a short (5−6 cm) column of activated alumina prior to use. The "cold" solvents used to wash isolated products were typically cooled to −30 °C before use. Thermolyses were typically conducted in sealed NMR tubes in an oil bath maintained at the specified temperature. In all preparations Ar = 2,6-$C_6H_3{}^iPr_2$.

Physical Measurements. ^1H (250 MHz) and ^{13}C (62.9 MHz) NMR spectra were recorded at probe temperature (unless otherwise specified) on a Bruker AM-250 or Varian Unity 300 spectrometer in C_6D_6 or toluene-d_8 solvent. Chemical shifts are referenced to protio impurities (δ 7.15 (C_6D_6), 2.09 (toluene-d_8)) or solvent ^{13}C resonances (δ 128.0 (C_6D_6), 20.4 (toluene-d_8)) and are reported downfield of Me_4Si. Carbon assignments were assisted by APT or gated $^{13}C\{^1H\}$ decoupled spectra. For ^1H and ^{13}C NMR assignments, numbering of the ring positions follows that shown in Figure 2, i.e. Ta[=N^5C^tBu=$^4CH^3C^tBu$=$^2CH^1C^t$-BuR] for the metallacycles and Ta[$\eta^2(N,C)$-N^5C^tBu=$^4CH^3C^tBu$=$^2CH^1C^t$-Bu] for the η^2-tri-*tert*-butylpyridine ligand. Electron ionization mass spectra (70 eV) were recorded to m/z = 999 on a Hewlett Packard 5970 mass selective detector and RTE-6/VM data system. For GC−mass spectra, the sample was introduced into the mass spectrometer by a Hewlett Packard model 5890 gas chromatograph equipped with an HP-5 column. Microanalytical samples were handled under nitrogen and were combusted with WO_3 (Desert Analytics, Tucson, AZ).

Starting Materials. [$\eta^2(N,C)$-2,4,6-$NC_5{}^tBu_3H_2$]Ta$(OAr)_2Cl$ (**1**) and 1,3,5-$NC_5{}^tBu_3H_2$ were prepared as previously described.[40] [$\eta^2(N,C)$-2,4,6-$NC_5{}^tBu_3D_2$]Ta$(OAr)_2Cl$ (**1-d_2**) was prepared in a manner analogous to the preparation of **1** by substituting $^tBuC{\equiv}CD$ in place of $^tBuC{\equiv}CH$ in the procedure.[40] $LiBEt_3H^*$ (H* = H or D; 1 M in THF), MeMgCl (3 M in THF), CD_3MgI (3 M in THF), EtMgCl (2 M in Et_2O), ^nPrMgCl (2 M in Et_2O), ^iPrMgCl (2 M in THF), ^nBuLi (1.6 M in hexanes), ^tBuLi (1.7 M in pentane), $^{13}CH_3I$, and neohexene were obtained from Aldrich and were used as received. $^{13}CH_3MgI$ was prepared as a 1 M THF solution from reacting $^{13}CH_3I$ and 2 equiv of Mg in the appropriate volume of THF and used without further purification or standardization. $LiCH_2SiMe_3$ was prepared by the literature method.[74] Ethylene was passed through a column of activated 4 Å molecular sieves and activated Ridox catalyst (supported Cu) prior to use.

Preparations. Ta(=NC^tBu=CHC^tBu=$CHCH^tBu$)$(OAr)_2$ (2). A solution of $LiBEt_3H$ (1 M in THF, 0.61 mL, 0.61 mmol) was added dropwise to a rapidly stirred, dark red solution of [$\eta^2(N,C)$-2,4,6-$NC_5{}^tBu_3H_2$]Ta$(OAr)_2Cl$ (**1**, 0.500 g, 0.611 mmol) in THF (ca. 20 mL). After 20 h at room temperature, the reaction volatiles were removed in *vacuo* to afford a red oil that was subsequently dissolved in cold pentane (ca. 20 mL) and filtered through Celite to remove the fine white precipitate that formed upon pentane addition. The Celite was washed with additional cold pentane (ca. 40 mL) until the washings were colorless. The combined orange filtrate and washings were concentrated to 1−2 mL in *vacuo* and cooled to −40 °C. After 2 days, the orange crystals that had formed were collected on a frit and dried *in vacuo* to provide 0.142 g (0.181 mmol or 30%) of **2** as an analytically pure, orange crystalline solid. While **2** is formed in nearly 50% yield, its extreme solubility has precluded its isolation in more than ca. 30% yield. ^1H NMR (C_6D_6): δ 7.11 and 6.98 (pseudo d and t, respectively (A_2B mult), 6 H total, H_{aryl}, OAr), 5.91 (s, 1 H, C(4)H), 5.84 (d, $^3J_{HH}$ = 10.5 Hz, 1 H, C(2)H), 4.51 (d, $^3J_{HH}$ = 10.5 Hz, 1 H, C(1)H), 3.97 and 3.81 (spt, 2 H each, $CHMe_2$), 1.36−1.24 (four overlapping d, 6 H each, $CHMe_2$), 1.28, 1.10, and 0.98 (s, 9 H each, CMe_3). ^{13}C NMR (C_6D_6, selected C−H coupling constants reported): δ 169.6 and 167.4 ($C(3)CMe_3$ and $C(5)CMe_3$), 158.5 and 156.4 (C_{ipso}), 138.8 and 136.3 (C_o), 123.4 (d of m, $^1J_{CH}$ = 160 Hz, C_p), 122.3 (d, $^1J_{CH}$ = 160 Hz, C_m), 116.7 (d of d, $^1J_{CH}$ = 153.9 Hz, C(4)H), 115.8 (d of m, $^1J_{CH}$ = 148.3 Hz, C(2)H), 103.4 (d of m, $^1J_{CH}$ = 135.0 Hz, $C(1)HCMe_3$), 38.7, 37.1, and 34.7 (CMe_3), 32.5, 30.4, and 29.1 (CMe_3), 27.1 and 26.9 ($CHMe_2$), 23.9, 23.7, 23.4, and 23.3 ($CHMe_2$). Anal. Calcd for $C_{41}H_{64}NO_2Ta$: C, 62.82; H, 8.23; N, 1.79. Found: C, 62.96; H, 8.14; N, 1.72.

Ta(=NC^tBu=CHC^tBu=$CHCD^tBu$)$(OAr)_2$ (2-d_1). This complex was prepared in an identical manner as its protio analog **2** using a 1 M THF solution of $LiBEt_3D$ rather than $LiBEt_3H$ in the preparation. Partial ^1H NMR (C_6D_6): δ 5.91 (s, 1 H, C(4)H), 5.84 (br s, 1 H, C(2)H); no signal is observed at δ 4.51 (C(1)D).

[$\eta^2(N,C)$-2,4,6-$NC_5{}^tBu_3H_2$]Ta$(OAr)_2Me$ (3). To a rapidly stirred, room temperature solution of [$\eta^2(N,C)$-2,4,6-$NC_5{}^tBu_3H_2$]Ta$(OAr)_2Cl$ (**1**, 0.500 g, 0.611 mmol) in benzene (ca. 10 mL) was added dropwise a solution of MeMgCl (3 M in THF, 0.203 mL, 0.611 mmol). Upon MeMgCl addition, the solution color immediately lightened from deep red to orange. This mixture was stirred for 15 min after which time the reaction volatiles were removed under reduced pressure to yield a red-orange oil. The oil was dissolved in cold pentane (ca. 20 mL) and filtered through Celite to remove the white solid which precipitated upon pentane addition. The pentane was removed from the orange filtrate in *vacuo* to provide the product as an orange oil. This oil was dissolved in a minimal volume of diethyl ether (ca. 2 mL), ca. 20 mL of acetonitrile was added, and the red-orange solution was cooled to −40 °C. After several hours, the small orange crystals that had formed were collected on a frit and dried in *vacuo*; yield 0.352 g (0.441 mmol, 72%) of **5** as an analytically pure product. ^1H NMR (C_6D_6, probe temperature): δ 7.06 and 6.94 (pseudo d and t, respectively (A_2B mult), 6 H total, H_{aryl}, OAr), 5.63 (br s, 2 H, H(2) and H(4)), 3.84 and 3.38 (br mult, 2 H, each, $CHMe_2$), 1.25−0.99 (overlapping s and d, 54 H total, $CHMe_2$, CMe_3, and $TaCH_3$). Partial ^1H NMR (toluene-d_8, −90 °C): δ 5.73 and 5.50 (H(2) and H(4)). ^{13}C NMR (C_6D_6): δ 170.4 (C(5), $NC_5{}^tBu_3H_2$), 158.0 (C_{ipso}, OAr), 150.2 (C(3), $NC_5{}^tBu_3H_2$), 137.7 (C_o, OAr), 123.7, 123.6, and 123.3 (C_m and C_p, OAr), 112.4 (C(1), $NC_5{}^tBu_3H_2$), 105.1 (C(2), $NC_5{}^tBu_3H_2$), 100.1 (C(4), $NC_5{}^tBu_3H_2$), 48.1 ($TaCH_3$), 41.5, 37.7, and 34.6 (CMe_3), 29.5, 27.8, and 23.6 (CMe_3), 29.2 and 28.8 ($CHMe_2$), 24.8 ($CHMe_2$). Anal. Calcd for $C_{42}H_{66}NO_2Ta$: C, 63.22; H, 8.34; N, 1.76. Found: C, 62.71; H, 8.34; N, 1.76.

[η^2(N,C)-2,4,6-$NC_5{}^tBu_3D_2$]Ta$(OAr)_2Me$ (3-d_2). This complex is prepared in a manner similar to its protio analog **3**, except [$\eta^2(N,C)$-2,4,6-$NC_5{}^tBu_3D_2$]Ta$(OAr)_2Cl$ (**1-d_2**) is substituted for unlabeled **1** in the procedure. ^1H NMR (C_6D_6, probe temperature): identical to that of **3** except that no signal is observed for the equilibrating pyridine ring protons (H(2) and H(4)) at δ 5.63.

(72) Shriver, D. F.; Drezdzon, M. A. *The Manipulation of Air-Sensitive Compounds*, 2nd ed; John Wiley and Sons: New York, 1986.

(73) Perrin, D. D.; Armarego, W. L. F. *Purification of Laboratory Chemicals*, 3rd ed; Pergamon Press: Oxford, 1988.

(74) Schrock, R. R.; Fellman, J. D. *J. Am. Chem. Soc.* **1978**, *100*, 3359.

[η²(*N,C*)-2,4,6-NC$_5$^{t}Bu$_3$H$_2$]Ta(OAr)$_2$(CD$_3$) (3-*d*$_3$). This complex is prepared in an identical manner and comparable yield as its protio analog **3** except that CD_3MgI (3 M in THF) was used in place of unlabeled MeMgCl in the preparation. ^{1}H NMR (C_6D_6, probe temperature): identical to that of complex **3** except the signal for the TaMe hydrogens at δ 1.17 is absent.

[η²(*N,C*)-2,4,6-NC$_5$^{t}Bu$_3$H$_2$]Ta(OAr)$_2$(^{13}CH$_3$) (3-^{13}C). This complex is prepared in an identical manner and comparable yield as the unlabeled methyl analog **3** except that $^{13}CH_3MgI$ (1 M in THF) was substituted for the unlabeled MeMgCl in the preparation. ^{1}H NMR (C_6D_6, probe temperature): identical to that of the **3** except the signal for the Ta$^{13}CH_3$ hydrogens appears as a δ 1.17 doublet ($^1J_{CH}$ = 121.5 Hz).

[η²(*N,C*)-2,4,6-NC$_5$^{t}Bu$_3$D$_2$]Ta(OAr)$_2$(^{13}CH$_3$) (3-^{13}C,*d*$_2$). This complex is prepared in a manner similar to its unlabeled analog **3**, except that both [η²(*N,C*)-2,4,6-$NC_5{}^tBu_3D_2$]Ta(OAr)$_2$Cl (**1**-*d*$_2$) and $^{13}CH_3MgI$ (1 M in THF) were employed in the preparation. ^{1}H NMR (C_6D_6, probe temperature): identical to that of **3** except the signal for the methyl group appears as a δ 1.17 doublet ($^1J_{CH}$ = 121.5 Hz) and the signals for the pyridine ring protons (H(2) and H(4)) at δ 5.63 are absent.

[η²(*N,C*)-2,4,6-NC$_5$^{t}Bu$_3$H$_2$]Ta(OAr)$_2$Et (4). A solution of EtMgBr (2 M in Et_2O, 0.611 mL, 1.22 mmol) was added dropwise to a rapidly stirred benzene solution of [η²(*N,C*)-2,4,6-$NC_5{}^tBu_3H_2$]Ta(OAr)$_2$Cl (**1**, 1.000 g, 1.22 mmol) in 10 mL of benzene, whereupon the solution slowly lightened from dark red to orange. After 20 h, this reaction was worked up in a manner analogous to the methyl complex **3**. After the Et_2O/NCMe solution was stored at −40 °C for 20 h, beautiful red orange crystals had formed leaving behind a nearly decolorized, yellow orange mother liquor. The crystals were collected on a frit and dried in *vacuo* to provide 0.752 g (0.926 mmol, 76%) of **4** as analytically pure, red orange crystals. ^{1}H NMR (C_6D_6): δ 7.07−6.95 (A_2B mult, 6 H total, H_{aryl}, OAr), 5.84 (s, 1 H, H(2)), 5.70 (s, 1 H, H(4)), 3.82 and 3.40 (br spt, 2 H each, C*H*Me$_2$), 1.98−1.92 (mult, 3 H, CH_2CH_3),.1.84−1.78 (mult, 2 H, CH_2CH_3), 1.34−0.98 (overlapping s and d, 51 H total, CH*Me*$_2$ and C*Me*$_3$ groups). ^{13}C NMR (C_6D_6): δ 169.5 (C(5), $NC_5{}^tBu_3H_2$), 158.2 and 157.8 (C_{ipso}, OAr), 149.5 (C(3), $NC_5{}^tBu_3H_2$), 138.0 (C_o, OAr), 123.8, 123.5 and 123.3 (C_m and C_p, OAr), 112.1 (C(1), $NC_5{}^tBu_3H_2$), 108.0 (C(2), $NC_5{}^tBu_3H_2$), 101.1 (C(4), $NC_5{}^tBu_3H_2$), 64.1 (*C*H$_2$CH$_3$), 41.7, 37.6, and 34.8 (*C*Me$_3$), 30.2, 29.4, and 28.9 (C*Me*$_3$), 27.5 and 27.3 (*C*HMe$_2$), 24.8, 24.1, 24.0, and 23.8 (CH*Me*$_2$), 15.1 (CH$_2$*C*H$_3$). Anal. Calcd for $C_{43}H_{68}NO_2Ta$: C, 63.61; H, 8.44; N, 1.72. Found: C, 63.82; H, 8.31; N, 1.72.

[η²(*N,C*)-2,4,6-NC$_5$^{t}Bu$_3$H$_2$]Ta(OAr)$_2$^{n}Pr (5). To a rapidly stirred benzene solution of [η²(*N,C*)-2,4,6-$NC_5{}^tBu_3H_2$]Ta(OAr)$_2$Cl (**1**, 0.250 g, 0.306 mmol) in 10 mL of benzene was added dropwise a solution of ^{n}PrMgCl (2 M in Et_2O, 0.153 mL, 0.306 mmol). The solution slowly lightened from dark red to orange after ^{n}PrMgCl addition and was subsequently allowed to stir for 2 h. After this time, the reaction was worked up in a manner analogous to the methyl complex **3**, except that the Et_2O/NCMe solution of **5** was allowed to stand at room temperature for several hours. Over this time, lovely red orange crystals were seen to form. After ca. 18 h, the product was filtered off from the nearly decolorized, yellow orange mother liquor and dried in *vacuo* to provide 0.154 g (0.186 mmol, 61%) of **5** as analytically pure, orange crystals. ^{1}H NMR (C_6D_6): δ 7.06−6.94 (br A_2B mult, 6 H, H_{aryl}, OAr), 5.84 (s, 1 H, H(2)), 5.69 (s, 1 H, H(4)), 3.83 and 3.39 (br spt, 2 H, C*H*Me$_2$), 2.00 (mult, 2 H, $CH_2CH_2CH_3$), 1.79 (mult, 2 H, CH_2CH_2-CH_3), 1.35, 1.21, and 0.98 (s, 9 H each, C*Me*$_3$), 1.28−1.11 (overlapping d, 24 H total, CH*Me*$_2$), 1.01 (t, 3 H, $CH_2CH_2CH_3$). ^{13}C NMR (C_6D_6): δ 169.7 (C(5), $NC_5{}^tBu_3H_2$), 158.2 and 157.8 (C_{ipso}, OAr), 149.5 (C(3), $NC_5{}^tBu_3H_2$), 138.0 (C_o, OAr), 123.9, 123.6, and 123.3 (C_m and C_p, OAr), 112.2 (C(1), $NC_5{}^tBu_3H_2$), 107.9 (C(2), $NC_5{}^tBu_3H_2$), 101.1 (C(4), $NC_5{}^tBu_3H_2$), 74.6 (*C*H$_2$CH$_2$CH$_3$), 41.7, 37.6, and 34.7 (*C*Me$_3$), 30.1, 29.4, and 28.9 (C*Me*$_3$), 27.5 and 27.3 (*C*HMe$_2$), 24.8, 24.2, 24.0, and 23.8 (CH*Me*$_2$), 24.5 (CH$_2$*C*H$_2$CH$_3$), 21.8 (CH$_2$CH$_2$*C*H$_3$). Anal. Calcd for $C_{44}H_{70}NO_2Ta$: C, 63.98; H, 8.54; N, 1.70. Found: C, 63.99; H, 8.48; N,1.75.

[η²(*N,C*)-2,4,6-NC$_5$^{t}Bu$_3$H$_2$]Ta(OAr)$_2$^{n}Bu (6). A solution of ^{n}BuLi (1.6 M in hexanes, 0.191 mL, 0.306 mmol) was added dropwise to a rapidly stirred benzene solution of [η²(*N,C*)-2,4,6-$NC_5{}^tBu_3H_2$]Ta(OAr)$_2$-Cl (**1**, 0.250 g, 0.306 mmol) in 10 mL of benzene. A gradual change in the solution color from dark red to orange was observed and after 4 h, the reaction was worked up in a manner analogous to the methyl complex **3**, except that the Et_2O/NCMe solution of **6** was allowed to stand at room temperature. Beautiful orange crystals were seen to form after several minutes, and after 24 h, the crystals were collected by filtration and dried in *vacuo* to provide 0.165 g (0.196 mmol, 64%) of **6** as analytically pure, orange crystalline solid. ^{1}H NMR (C_6D_6): δ 7.06−6.83 (br A_2B mult, 6 H, H_{aryl}, OAr), 5.84 (s, 1 H, H(2)), 5.70 (s, 1 H, H(4)), 3.83 and 3.38 (br spt, 2 H, C*H*Me$_2$), 2.10−1.61 (overlapping br mult, 4 H total, $CH_2CH_2CH_2CH_3$ and $CH_2CH_2CH_2CH_3$), 1.36, 1.21, and 0.98 (s, 9 H each, C*Me*$_3$), 1.28−1.11 (overlapping d and mult, 26 H total, $CH_2CH_2CH_2Me$ and CH*Me*$_2$), 0.92 (t, 3 H, $CH_2CH_3CH_2CH_3$). ^{13}C NMR (C_6D_6): δ 169.7 (C(5), $NC_5{}^tBu_3H_2$), 158.2 and 157.8 (C_{ipso}, OAr), 149.5 (C(3), $NC_5{}^tBu_3H_2$), 138.1 (C_o, OAr), 123.9, 123.6, and 123.3 (C_m and C_p, OAr), 112.3 (C(1), $NC_5{}^tBu_3H_2$), 107.9 (C(2), $NC_5{}^tBu_3H_2$), 101.1 (C(4), $NC_5{}^tBu_3H_2$), 72.0 (*C*H$_2$CH$_2$CH$_2$CH$_3$), 41.7, 37.6, and 34.8 (*C*Me$_3$), 32.8 (CH$_2$*C*H$_2$CH$_2$CH$_3$), 30.4, 30.1, and 29.4 (C*Me*$_3$), 28.9 (CH$_2$CH$_2$*C*H$_2$CH$_3$), 27.5 and 27.3 (*C*HMe$_2$), 24.9, 24.2, 24.1, and 23.8 (CH*Me*$_2$), 13.9 (CH$_2$CH$_2$CH$_2$*C*H$_3$). Anal. Calcd for $C_{45}H_{72}NO_2Ta$: C, 64.34; H, 8.64; N, 1.67. Found: C, 64.17; H, 8.82; N, 1.81.

[η²(*N,C*)-2,4,6-NC$_5$^{t}Bu$_3$H$_2$]Ta(OAr)$_2$(CH$_2$SiMe$_3$) (7). A solution of $LiCH_2SiMe_3$ (1 M in THF, 0.610 mL, 0.610 mmol) was added dropwise to a rapidly stirring benzene solution of [η²(*N,C*)-2,4,6-$NC_5{}^tBu_3H_2$]Ta(OAr)$_2$Cl (**1**, 0.500 g, 0.610 mmol) in 10 mL of benzene. A gradual change in the solution color from dark red to orange was observed, and after 2 h, the reaction was worked up in a manner analogous to the methyl complex **3**, except that the Et_2O/NCMe solution of **7** was allowed to stand at room temperature. After several minutes, lovely orange crystals were seen to form, and after 24 h, these crystals were collected by filtration and dried *in vacuo* to provide 0.402 g (0.462 mmol, 76%) of **7** as analytically pure orange crystals. ^{1}H NMR (C_6D_6): δ 7.10−6.91 (A_2B mult, 6 H total, H_{aryl}, OAr), 5.85 (s, 1 H, H(2)), 5.66 (s, 1 H, H(4)), 3.82 and 3.31 (br spt, 2 H each, C*H*Me$_2$), 1.37−0.90 (overlapping mult, 53 H total, C*H*$_2$SiMe$_3$, CH*Me*$_2$, and C*Me*$_3$), 0.20 (s, 9 H, CH$_2$*Me*$_3$). ^{13}C NMR (C_6D_6): δ 171.2 (C(5), $NC_5{}^tBu_3H_2$), 158.5 and 157.6 (C_{ipso}, OAr), 148.2 (C(3), $NC_5{}^tBu_3H_2$), 138.2 (C_o, OAr), 124.1, 123.9, and 123.4 (C_m and C_p, OAr), 112.6 (C(1), $NC_5{}^tBu_3H_2$), 107.9 (C(2), $NC_5{}^tBu_3H_2$), 100.2 (C(4), $NC_5{}^tBu_3H_2$), 62.7 (*C*H$_2$SiMe$_3$), 41.8, 37.8, and 34.8 (*C*Me$_3$), 29.9, 29.5, and 28.9 (C*Me*$_3$), 27.2 and 26.9 (*C*HMe$_2$), 25.1, 24.9, 24.6, and 24.3 (CH*Me*$_2$), 3.32 (CH$_2$Si*Me*$_3$). Anal. Calcd for $C_{45}H_{74}NO_2SiTa$: C, 62.12; H, 8.57; N, 1.61. Found: C, 62.08; H, 8.78; N, 1.47.

Ta(=NC^{t}Bu=CHC^{t}Bu=CHC^{t}BuMe)(OAr)$_2$ (8). In a typical experiment, an orange solution of [η²(*N,C*)-2,4,6-$NC_5{}^tBu_3H_2$]Ta(OAr)$_2$-Me (**3**, 0.040 g, 0.050 mmol) in 0.50 mL of C_6D_6 was sealed in an NMR tube and heated to 80 °C in an oil bath. After 36 h, the ^{1}H NMR spectrum of the mixture was recorded. In addition to some starting material **3** that remained unreacted, resonances assigned to new complex **8** were observed. Partial ^{1}H NMR (C_6D_6): δ 6.36 (br s, H(2)), 6.05 (s, H(4)), 3.95 and 3.75 (spt, C*H*Me$_2$), 3.17 (s, C*H*$_3$). This complex has not been induced to crystallize from the reaction mixture and has therefore not been isolated in a pure fashion.

Ta(=NC^{t}Bu=CDC^{t}Bu=CDC^{t}BuMe)(OAr)$_2$ (8-*d*$_2$). This complex is prepared in a manner identical to its protio analog **8** except that **3**-*d*$_2$ is employed in the thermolysis in place of unlabeled **3**. Partial ^{1}H NMR (C_6D_6): δ 3.95 and 3.75 (spt, C*H*Me$_2$), 3.17 (s, C$_\alpha$C*H*$_3$). No signals assignable to H(2) or H(4) were observed at δ 6.36 or 6.05.

Ta(=NC^{t}Bu=CHC^{t}Bu=CHC^{t}BuCD$_3$)(OAr)$_2$ (8-*d*$_3$). This complex is prepared in a manner similar to its protio analog **8** except that **3**-*d*$_3$ is employed in the thermolysis in place of unlabeled **3**. Partial ^{1}H NMR (C_6D_6): δ 6.36 (br s, H(2)), 6.05 (s, H(4)), 3.95 and 3.75 (spt, C*H*Me$_2$). No signal assignable to C$_\alpha$C*H*$_3$ was observed at δ 3.17.

Ta(=NC^{t}Bu=CHC^{t}Bu=CHC^{t}Bu^{13}CH$_3$)(OAr)$_2$ (8-^{13}C). This complex is prepared in a manner similar to its protio analog **8** except that **3**-^{13}*C* is employed in the thermolysis in place of unlabeled **3**. Partial ^{1}H NMR (C_6D_6): δ 6.36 (d, $^3J_{CH}$ = 3.3 Hz, H(2)), 6.05 (s, H(4)), 3.95 and 3.75 (spt, C*H*Me$_2$), 3.17 (d, $^1J_{CH}$ = 126 Hz, C$_\alpha$13C*H*$_3$).

Ta(=NC^{t}Bu=CHC^{t}Bu=CHC^{t}BuR)(OAr)$_2$ [R = Et (9), ^{n}Pr (10), ^{n}Bu (11)]. Complexes **9**−**11** were all generated in procedures

analogous to that described for **8** by thermolysis of the appropriate $[\eta^2(N,C)$-2,4,6-$NC_5{}^tBu_3H_2]Ta(OAr)_2R$ [R = Et (**4**), ^{n}Pr (**5**), or ^{n}Bu (**6**)] complex at 80 °C in C_6D_6. Spectra were typically recorded after 36 h. Partial ^{1}H NMR (C_6D_6) data for these complexes are recorded in Table 4.

$Ta(=NC^tBu=CHC^tBu=CHC^tBuHCH_2)(OAr)_2$ (12). This species was detected in minor concentrations in the thermolysis of **3** (125 °C, 4 h) in a sealed NMR tube in C_6D_6. Significant amounts of $Ta(=NC^tBu=CHC^tBu=CHC^tBuMe)(OAr)_2$ (**8**), a small amount of unreacted $[\eta^2(N,C)$-2,4,6-$NC_5{}^tBu_3H_2]Ta(OAr)_2Me$ (**3**), and *tert*-butylethylene were also observed by NMR in this solution. Partial ^{1}H NMR (C_6D_6): δ 5.55 (s, 1 H, H(4)), 5.50 (d, $^3J_{HH}$ = 10.5 Hz, 1 H, H(2)), 2.93 (mult, 1 H, H(1c)), 2.50 (mult, 1 H, H(1a)), 1.90 (mult, 1 H, H(1b)).

$Ta(=NC^tBu=CHC^tBu=CHC^tBuDCD_2)(OAr)_2$ (12-d_3). This complex was detected in minor concentrations in the thermolysis of **3-d_2** at 125 °C for 4 h as described in the observation of **12**. Partial ^{1}H NMR (C_6D_6): δ 5.55 (s, 1 H, H(4)), 5.50 (br s, 1 H, H(2)). No signals assignable to H(1a), H(1b), or H(1c) were observed at δ 2.93, 2.50, or 1.90.

$Ta(=NC^tBu=CHC^tBu=CHC^tBuH^{13}CH_2)(OAr)_2$ (12-^{13}C). This complex was detected in minor concentrations upon thermolyzing **3-^{13}C** at 125 °C for 4 h as described in the observation of **12**. Partial ^{1}H NMR (C_6D_6): the δ 2.93, 2.50, or 1.90 signals assigned to H(1a), H(1b), or H(1c) were further split into more complex multiplets from ^{13}C coupling and the H(2) signal was broadened.

$Ta(=NC^tBu=CHC^tBu=CHC^tBuHCH_2)(OAr)_2\cdot 2NCMe$ (12-NCMe). A large Schlenk tube (Teflon stopcock) was charged with 0.600 g (0.752 mmol) of $[\eta^2(N,C)$-2,4,6-$NC_5{}^tBu_3H_2]Ta(OAr)_2Me$ (**3**), 40 mL of benzene, and excess PMe_3 (0.500 mL, 4.83 mmol). The tube was sealed and the reaction mixture was stirred at reflux in a 100 °C oil bath for 3 days over which time the solution color became deep red in color. After this time, the mixture was cooled to room temperature and the reaction volatiles were removed under reduced pressure to provide a red oil. This oil was taken up in a minimal volume of Et_2O (ca. 2 mL), acetonitrile (ca. 15 mL) was added whereupon the solution color quickly lightened to orange, and the mixture was cooled to −40 °C. After 3 days, the colorless crystals which had formed were collected by filtration and dried in *vacuo* to provide 0.373 g (0.419 mmol, 58%) of **12-NCMe** as a white solid. ^{1}H NMR (C_6D_6): δ 7.23−7.14 (mult, 4H, H_m, OAr), 7.02−6.95 (mult, 2 H, H_p, OAr), 5.53 (s, 1 H, H(4)), 5.49 (d, $^3J_{CH}$ = 10.5 Hz), 3.80 and 3.57 (spt, 2 H each, C*H*Me_2), 2.96 (mult, 1 H, H(1c)), 2.35 (mult, 1 H, H(1a)), 1.76 (mult, 1 H, H (1b)), 1.48−1.30 (set of four overlapping d, 24 H total, CH*Me*$_2$), 1.15, 1.14, and 0.959 (s, 9 H each, CMe_3), and 0.440 (s, 6 H, MeCN). This complex appears to lose coordinated acetonitrile slowly over time and more rapidly under vacuum. Therefore the elemental analysis of this complex is consistent with 1.6−1.7 equiv of NCMe per tantalum rather than 2 equiv predicted from the ^{1}H NMR data. Anal. Calcd for $C_{47}H_{70}N_3O_2Ta$ (which includes 2NCMe): C, 63.43; H, 7.93; N, 4.72. Found: C, 62.68; H, 8.49, N, 4.27.

$[Ta(\mu$-$NC^tBu=CHC^tBu=CH)(OAr)_2]_2$ (13). (i) **From $[\eta^2(N,C)$-2,4,6-$NC_5{}^tBu_3H_2]Ta(OAr)_2Me$ (3).** An ampule (Teflon stopcock) was charged with 0.250 g (0.313 mmol) of $[\eta^2(N,C)$-2,4,6-$NC_5{}^tBu_3H_2]$-$Ta(OAr)_2Me$ (**3**) and 50 mL of benzene. The stopcock was sealed and the reaction mixture was stirred at reflux in a 140 °C oil bath for 10 days over which time the solution color slowly faded and orange crystals were seen to form. After this time the solution had almost entirely decolorized. The mixture was allowed to cool to room temperature and the orange crystals which had formed were collected by filtration, washed with pentane (ca. 40 mL) followed by benzene (ca. 20 mL), and dried *in vacuo*. This procedure afforded 0.180 g (0.144 mol, 92%) of **13** as an analytically pure orange solid. Anal. Calcd for $C_{72}H_{108}N_2O_4Ta_2$: C, 60.58; H, 7.63; N, 1.96. Found: C, 60.63; H, 7.71; N, 1.93.

(ii) **From $[\eta^2(N,C)$-2,4,6-$NC_5{}^tBu_3H_2]Ta(OAr)_2R$ [R = Et (4), ^{n}Pr (5), ^{n}Bu (6)].** Complex **13** was also obtained in high yield from the thermal decomposition of complexes **4**, **5**, and **6**. In these preparations, 0.5 mL of a solution of **4**, **5**, or **6** (0.1 M in C_6D_6, 0.05 mmol) was thermolyzed at 80 °C in a sealed NMR tube for 3 weeks. After this time, the tube was broken, the resulting orange crystals were collected by decanting the supernatent, and this clear yellow supernatent was examined by GC−mass spec analysis to determine the alkene produced. The crystals were washed with benzene (ca. 10 mL) to provide **13** in ca. 85−90% yield. The assignment of this very insoluble sample as complex **13** was made by comparing the unit cell from X-ray crystallographic data and from the fingerprint IR data (KBr pellet).

Experiments. Attempts to Isolate $[\eta^2(N,C)$-2,4,6-$NC_5{}^tBu_3H_2]$-$Ta(OAr)_2H$. Since the pyridine ligand in $[\eta^2(N,C)$-2,4,6-$NC_5{}^tBu_3H_2]Ta(OAr)_2Cl$ (**1**) is assembled at the metal center by a cyclotrimerization reaction,[40] efforts were made to produce a hydride complex of one of the precursor species. If a species such a $Ta(C^tBu=CHCH=C^tBu)(OAr)_2(H)$ or $Ta(C^tBu=CHC^tBu=CH)(OAr)_2(H)$ could be prepared, then further cycloaddition with 1 equiv of ^{t}BuC≡N would afford the desired $\eta^2(N,C)$-pyridine hydride complex. Reaction of either metallacycle $Ta(C^tBu=CHCH=C^tBu)(OAr)_2Cl$ or $Ta(C^tBu=CHC^tBu=CH)(OAr)_2Cl$ with $LiBEt_3H$, Et_3SiH, or $^nBu_3SnH$ provided only starting material or uncharacterizable mixtures of products. The reaction of the ethyl derivative, $[\eta^2(N,C)$-2,4,6-$NC_5{}^tBu_3H_2]Ta(OAr)_2Et$ (**4**), with hydrogen (1000 psi) also failed to provide any of the possible hydrogenolysis products. This reaction afforded mostly starting material along with a trace amount of free tri-*tert*-butylpyridine as the only spectroscopically identifiable species.

Ring-Rocking studies of $[\eta^2(N,C)$-2,4,6-$NC_5{}^tBu_3H_2]Ta(OAr)_2Me$ (3). (i) A solution of $[\eta^2(N,C)$-2,4,6-$NC_5{}^tBu_3D_2]Ta(OAr)_2Me$ (**3-d_2**, 0.035 g, 0.044 mmol) and free tri-*tert*-butylpyridine (0.010 g, 0.040 mmol) was prepared in 5 mL of C_6D_6 and the ^{1}H NMR spectrum of the solution was examined within several minutes. No signal at δ 5.63 corresponding to the C(2) and C(4) resonances of the exchange product $[\eta^2(N,C)$-2,4,6-$NC_5{}^tBu_3H_2]Ta(OAr)_2Me$ (**3**) was observed. (ii) Excess pyridine (10 μL, 0.12 mmol, ca. 5 equiv) was added to a solution of $[\eta^2(N,C)$-2,4,6-$NC_5{}^tBu_3D_2]Ta(OAr)_2Me$ (**3-d_2**, 0.020 g, 0.025 mmol) in 5 mL of C_6D_6 and the ^{1}H NMR spectrum of the solution was examined within several minutes. Only resonances attributed to unreacted **3** and NC_5H_5 were observed. (iii) The crossover experiments described in the text also rule out a dissociative equilibration of H(2) and H(4) observed in the ^{1}H NMR. Thus, an equimolar mixture of $[\eta^2(N,C)$-2,4,6-$NC_5{}^tBu_3D_2]Ta(OAr)_2Me$ (**3-d_2**) and $[\eta^2(N,C)$-2,4,6-$NC_5{}^tBu_3H_2]Ta(OAr)_2(^{13}CH_3)$ (**3-^{13}C**) was thermolyzed (C_6D_6 sealed tube, 120 °C, 4 h) and the resulting solution observed by ^{1}H NMR. Only $Ta(=NC^tBu=CDC^tBu=CDC^tBuMe)(OAr)_2$ (**8-d_2**) and $Ta(=NC^tBu=CHC^tBu=CHC^tBu^{13}CH_3)(OAr)_2$ (**8-^{13}C**) were present in the sample. Thermolyzing an equimolar mixture of $[\eta^2(N,C)$-2,4,6-$NC_5{}^tBu_3H_2]Ta(OAr)_2Me$ (**3**) and $[\eta^2(N,C)$-2,4,6-$NC_5{}^tBu_3D_2]$-$Ta(OAr)_2(^{13}CH_3)$ (**3-$^{13}C,d_2$**) under similar conditions affords only $Ta(=NC^tBu=CHC^tBu=CHC^tBuMe)(OAr)_2$ (**8**) and $Ta(=NC^tBu=CDC^tBu=CDC^tBu^{13}CH_3)(ArO)_2$ (**8-$^{13}C,d_2$**).

Reaction of $[\eta^2(N,C)$-2,4,6-$NC_5{}^tBu_3H_2]Ta(OAr)_2Cl$ (1) with ^{t}BuLi. A portion of ^{t}BuLi (36 μL of a 1.7 M pentane solution, 0.061 mmol) was added to a stirred solution of $[\eta^2(N,C)$-2,4,6-$NC_5{}^tBu_3H_2]Ta(OAr)_2$-Cl (**1**, 0.050 g, 0.061 mmol) in 5 mL of benzene. This mixture was stirred at room temperature for 2 h after which time the reaction volatiles were removed in vacuo to afford an orange solid. The product was extracted from this solid with pentane, the extract was filtered through Celite, and the solvent was removed from the filtrate under reduced pressure to provide an orange solid. A C_6D_6 solution of this solid was prepared and examined by ^{1}H NMR and shown to consist primarily of $Ta(=NC^tBu=CHC^tBu=CHCH^tBu)(OAr)_2$ (**2**), with free 2,4,6-$NC_5{}^tBu_3H_2$ and other unidentified decomposition products also being present.

Reaction of $[\eta^2(N,C)$-2,4,6-$NC_5{}^tBu_3H_2]Ta(OAr)_2Cl$ (1) with ^{t}PrMgCl. To a stirred solution of $[\eta^2(N,C)$-2,4,6-$NC_5{}^tBu_3H_2]Ta(OAr)_2$-Cl (**1**, 0.500 g, 0.611 mmol) in 10 mL of C_6H_6 was added ^{i}PrMgCl (0.306 mL of a 2 M THF solution, 0.611 mmol). This mixture was stirred for 2 h after which the reaction volatiles were removed under vacuum to afford a red oil. The product was extracted from this oil

with cold (−35 °C) pentane, the extract was filtered through Celite, and the solvent was removed from the filtrate in vacuo to afford an orange red oil. Crystals of product (0.203 g, 0.246 mmol, 40%) were obtained at −35 °C from Et_2O/NCMe solutions of this oil and were shown to be spectroscopically identical to [$\eta^2(N,C)$-2,4,6-$NC_5{}^tBu_3H_2$]Ta$(OAr)_2{}^nPr$ (**5**) that was prepared using ^nPrMgCl. At shorter reaction times (ca. 15 min), a substantial amount of a second product was observed after appropriate workup but could not be isolated. This complex was tentatively identified as the isopropyl derivative [$\eta^2(N,C)$-2,4,6-$NC_5{}^tBu_3H_2$]Ta$(OAr)_2{}^iPr$ based upon its ^1H NMR spectrum. Partial ^1H NMR (C_6D_6): δ 5.73 and 6.21 (s, H(2) and H(4)), 3.45 (partially obscured spt, C*H*Me_2), 1.9−2.1 (partially obscured mult).

Reaction of [$\eta^2(N,C)$-2,4,6-$NC_5{}^tBu_3H_2$]Ta$(OAr)_2$Cl (1) with ^iPrMgCl in the Presence of CH_2=CHCMe$_3$. Isopropyl magnesium chloride (31 μL of a 2 M THF solution, 0.062 mmol) was added to a stirred solution of [$\eta^2(N,C)$-2,4,6-$NC_5{}^tBu_3H_2$]Ta$(OAr)_2$Cl (**1**) (0.050 g, 0.061 mmol) and neohexene (80 μL, 0.62 mmol) in 5 mL of benzene. This mixture was stirred at room temperature for 2 h after which time the volatiles were removed under reduced pressure and the resulting orange solid redissolved in pentane. This pentane solution was filtered through Celite and the solvent removed from the filtrate *in vacuo* to afford an orange solid. A C_6D_6 solution of this solid was prepared and examined by ^1H NMR and shown to be [$\eta^2(N,C)$-2,4,6-$NC_5{}^tBu_3H_2$]Ta$(OAr)_2{}^nPr$ (**5**); no evidence for incorporation of neohexene was obtained.

Reaction of [$\eta^2(N,C)$-2,4,6-$NC_5{}^tBu_3H_2$]Ta$(OAr)_2$Cl (1) with ^tBuLi in the Presence of CH_2=CHCMe$_3$. To a solution of [$\eta^2(N,C)$-2,4,6-$NC_5{}^tBu_3H_2$]Ta$(OAr)_2$Cl (**1**) (0.050 g, 0.061 mmol) and neohexene (80 μL, 0.62 mmol) in 5 mL of benzene was added ^tBuLi (37 μL of a 1.7 M pentane solution, 0.063 mmol). This mixture was stirred at room temperature for 2 h after which time the volatiles were removed *in vacuo*. The product was extracted from the resulting orange solid with pentane and the pentane solution was filtered through Celite. An orange solid was obtained upon removing the solvent from the filtrate under reduced pressure. A C_6D_6 solution of this solid was prepared and examined by ^1H NMR and shown to consist of Ta(=NC^{t}Bu=CHC^{t}Bu=CHCH^{t}Bu)$(OAr)_2$ (**2**); no evidence for incorporation of neohexene was obtained.

Reaction of [$\eta^2(N,C)$-2,4,6-$NC_5{}^tBu_3H_2$]Ta$(OAr)_2$Cl (1) with ^tBuLi in Neat CH_2=CHCMe$_3$. To a stirred solution of [$\eta^2(N,C)$-2,4,6-$NC_5{}^tBu_3H_2$]Ta$(OAr)_2$Cl (**1**, 0.050 g, 0.061 mmol) in 2 mL of CH_2=CHCMe$_3$ was added a pentane solution of 1 equiv of ^tBuLi (37 μL of a 1.7 M pentane solution, 0.063 mmol). A precipitate (presumably LiCl) was seen to form over 15 min after which time the reaction volatiles were removed in *vacuo* and the resulting orange solid redissolved in pentane and filtered through Celite. The solvent was removed from the filtrate under reduced pressure to provide an orange solid. A C_6D_6 solution of this solid was prepared and examined by ^1H NMR and shown to consist of Ta(=NC^{t}Bu=CHC^{t}Bu=CHCH^{t}Bu)$(OAr)_2$ (**2**); no evidence for incorporation of neohexene was obtained.

Reaction of [$\eta^2(N,C)$-2,4,6-$NC_5{}^tBu_3H_2$]Ta$(OAr)_2$Cl (1) with ^tBuLi in the Presence of Ethylene. Ethylene was bubbled through a solution of [$\eta^2(N,C)$-2,4,6-$NC_5{}^tBu_3H_2$]Ta$(OAr)_2$Cl (**1**, 0.050 g, 0.061 mmol) in 25 mL of benzene for 5 min. To this stirred solution was added ^tBuLi (37 μL of a 1.7 M pentane solution, 0.063 mmol) in 1 mL of benzene. After this mixture was stirred for 30 min, the volatiles were removed under vacuum and the resulting yellow-orange solid was redissolved in pentane. This pentane solution was then filtered through Celite and the solvent removed from the filtrate *in vacuo* to provide a light orange solid. A C_6D_6 solution of this solid was prepared and examined by ^1H NMR and shown to consist of free 2,4,6-$NC_5{}^tBu_3H_2$ and other unidentified decomposition products.

X-ray Structural Determinations. Table 1 summarizes the crystal data and collection, solution, and refinement parameters for all three compounds examined. The space groups for compounds **2** and **4** were determined from the systematic absences and the subsequent least-squares refinement. The space group for **13** was determined by the lack of systematic absences and a subsequent density calculation that afforded the value of *Z*. Structures were solved by the Patterson method. All non-hydrogen atoms were refined anisotropically.

Structural Studies of Ta(=NC^{t}Bu=CHC^{t}Bu=CHCH^{t}Bu)$(OAr)_2$ (2). A red, plate-like crystal of **2** was crystallized from concentrated pentane solution at −35 °C and was mounted in a glass capillary in a random orientation. Hydrogen atoms of methyl groups were positioned by locating at least one hydrogen on each methyl group and generating missing hydrogen atoms and idealizing all methyl group hydrogens. Hydrogen atoms on the main backbone of the metallacycle [C(1), C(2), and C(4)] were located from difference maps. The remaining hydrogen atoms were included at idealized positions.

Structural Studies of [$\eta^2(N,C)$-2,4,6-$NC_5{}^tBu_3H_2$]Ta$(OAr)_2$Et (4). An orange, parallelpiped crystal of **4** was crystallized from Et_2O/acetonitrile (−35 °C) and mounted in a glass capillary in a random orientation. Hydrogen atoms were found in the difference maps but placed at idealized positions and subsequently included in the refinement. The hydrogen atoms bonded to C(8) were not located in the difference map and were not included in the refinement. Hydrogen atoms H(7A) and H(7B) were located from the difference map but were not idealized. Likewise, C(7) and C(8) were refined with fixed isotropic parameters since the ethyl was characterized by extreme thermal motion.

Structural Studies of [Ta(μ-NC^{t}Bu=CHC^{t}Bu=CH)$(OAr)_2]_2$ (13). A red, multifaceted block crystal of **13** was collected directly from the thermolysis reaction of **3** in benzene and was mounted on a glass fiber in a random orientation. Hydrogen positions were clearly visible in difference maps and hydrogens bonded to metallacyclic carbons C(33) and C(35) were added directly from a difference map. Methyl group carbons were added from difference maps, then idealized. Hydrogen atoms on all other carbon positions were added at idealized coordinates and were included in the refinement.

Acknowledgment is made to the Division of Chemical Sciences, Office of Basic Energy Sciences, Office of Energy Research, U.S. Department of Energy (DE-FG03-93ER14349) for support of this research. Thanks are due Mr. Mark Malcomson for obtaining the GC−mass spectral data.

Supporting Information Available: Details of the structure solution and refinement, including tables of crystal data and data collection parameters, atomic positional and thermal parameters, bond distances, bond angles, least-squares planes, and ORTEP figures for Ta(=NC^{t}Bu=CHC^{t}Bu=CHCH^{t}Bu)$(OAr)_2$ (**2**), [$\eta^2(N,C)$-2,4,6-$NC_5{}^tBu_3H_2$]Ta$(OAr)_2$Et (**4**), and [Ta(μ-NC^{t}Bu=CHC^{t}Bu=CH)$(OAr)_2]_2$ (**13**) (60 pages); tables of observed and calculated structure factor amplitudes (57 pages). This material is contained in libraries on microfiche, immediately follows this article in the microfilm version of the journal, can be ordered from the ACS, and can be downloaded from the Internet; see any current masthead page for ordering information and Internet access instructions.

JA951239W